Using MODIS data for mapping of water types within river plumes in the Great Barrier Reef, Australia: towards the production of river plume risk maps for reef and seagrass ecosystems.

Petus, Caroline[a]; da Silva, Eduardo Teixeira[a]; Devlin, Michelle[a]; Wenger, Amelia[a] and Álvarez-Romero, Jorge G[a,b]*

[a] Centre for Tropical Water and Aquatic Ecosystem Research, Catchment to Reef Research Group, James Cook University, Townsville, QLD 4811, Australia

[b] Australian Research Council Centre of Excellence for Coral Reef Studies, James Cook University, Townsville, QLD 4811, Australia

[*] Corresponding author: +61 7 4701 4680; caroline.petus@jcu.edu.au

Abstract

River plumes are the major transport mechanism for nutrients, sediments and other land-based pollutants into the Great Barrier Reef (GBR, Australia) and are a major threat to coastal and marine ecosystems such as coral reefs and seagrass. Understanding the spatial extent, frequency of occurrence, loads and ecological impacts of land-based pollutants discharged through river plumes is essential to drive catchment management actions. In this study, a framework to produce river plume risk maps for seagrass and corals, using supervised classification of MODIS Level 2 (L2) satellite products, is presented. Based on relevant L2 product thresholds, river plumes are classified into Primary, Secondary, and Tertiary water types, which represent distinct WQ parameters concentrations and combination. Annual water type maps are produced over three wet seasons (2010 to 2013) as a case of study. These maps provide a synoptic basis to assess the likelihood and magnitude of the risk of reduced coastal WQ associated with the river discharge (river plume risk) and in combination with sound knowledge of the regional ecosystems can serve as the basis to assess potential ecological impacts for coastal and marine GBR ecosystems. The methods described herein provide relevant and easily reproducible large-scale information for river plume risk assessment and management.

Key words: water quality, river plume, water types, risk maps, ecological impact, monitoring, Great Barrier Reef

1. Introduction

Stretching more than 2000 km along the Queensland coast, Australia, the Great Barrier Reef Marine Park (hereafter GBR; Fig. 1a) was inscribed on the World Heritage List in October 1981. With over 2900 coral reefs, it is the most extensive reef system in the world, also sheltering over 43000 km^2 of seagrass meadows (Brodie and Waterhouse, 2012). Despite the protected status and World Heritage listing, the GBR is under stress from three main threats associated with anthropogenic activities: over-harvesting of marine resources, climate change and land-based pollution (Brodie et al., 2008a; Fabricius, 2011; Pandolfi et al., 2003). Since European settlement, loads of pollutants delivered to

the GBR have escalated, with recent estimates indicating increases by around 5.5, 6 and 9 times when compared to annual pre-European loads of total suspended particulate matter, total nitrogen, and total phosphorus, respectively (Kroon et al., 2012). Discharge of pollutants to the GBR occurs mainly during the high-flow events associated with the north Queensland wet season between December to April (Devlin and Schaffelke, 2009).

River discharge carrying land-based pollutants result in both acute and chronic stress on coral reefs and seagrass beds due to the changes in water quality (WQ) conditions associated with the occurrence and duration of river flood plume formation (hereafter river plumes). Acute stresses on marine ecosystems are usually associated with extreme weather conditions resulting in prolonged exposure to low salinity river plumes, decreased light availability (due to suspended material) and high loads of pollutants (Devlin et al., 2011b, 2012a). Chronic stresses associated with increased levels of nutrients and turbidity can affect species susceptible to long-term changes in ambient environmental conditions (e.g., coral, seagrass and fish species; Brodie et al., 2012; Fabricius, 2005; Wenger and McCormick, 2013). The ecological impact of land-based pollutants transported in river plumes varies not only with the type of pollutant and the extent, frequency of occurrence and duration of the river plume, but also with the ecosystems being affected (e.g., McKenzie and Unsworth, 2011).

The use of remotely-sensed (RS) data in combination with in-situ sampling of WQ parameters during river plume events have improved our knowledge about composition, occurrence and extension of river plumes in the GBR coastal waters (e.g., Devlin et al., 2011a, 2012). Supervised methods based on classification of spectrally-enhanced quasi-true colour MODIS images have been proposed by Álvarez-Romero et al. (2013) to map river plumes in the GBR. Alternative methods have used Coloured Dissolved Organic Matter (CDOM) as an optical active constituent of river plumes, as well as combination of Level 2 (L2) products derived from MODIS satellite images (Devlin et al., 2012a) to delineate plume surface boundaries (Schroeder et al., 2012). These methods, in combination with pollutant loads, have been used to estimate acute or chronic exposure of GBR marine ecosystems to land-based pollutants (Álvarez-Romero et al., 2013; Devlin et al., 2012a, 2012b; Maughan and Brodie, 2009).

Based on in-situ WQ data, three river plume water types (hereafter water types) have been described from the inshore to the offshore boundary of river (e.g., Devlin et al., 2011b, 2012b). Each water type is associated with different levels and combination of pollutants (also identified as stressors) and hence will impact on different components of the GBR ecosystems (Devlin et al., 2012b). Identifying these water types can help clustering WQ stressors to assess river plume-related risk to the specific ecosystems. The next step towards the production of operational models of river plume-related risk (hereafter river plume risk) is thus to map the spatial extent, frequency and duration of the three water types within the river plume gradient. Devlin et al. (2012a) provided significant insights into how to incorporate MODIS L2 data to the monitoring of these three water types into the GBR lagoon. However, it has been identified that there is a need for further validation of these RS methods over a longer and repetitive time period and across different regions of the GBR (Devlin et al., 2012b; Devlin and Schaffelke, 2009).

Our study extends earlier work on monitoring water types in the GBR and tests the potential of MODIS L2 data over a multi-annual scale for mapping plume water types across the GBR. A

supervised method based on a combination of L2 satellite thresholds to delineate the different water types within GBR river plumes is proposed. The potential of using these maps to assess river plume risk to corals and seagrass ecosystems is then discussed. The main outcome of this work is a framework to provide relevant and easily reproducible large-scale information for river plume and water quality risk management.

2. Material and Methods

2.1. Study area

Our study focuses on the Great Barrier Reef, the world's largest coral reef system located in the Coral Sea, off the coast of Queensland in north-east Australia (Fig. 1a).

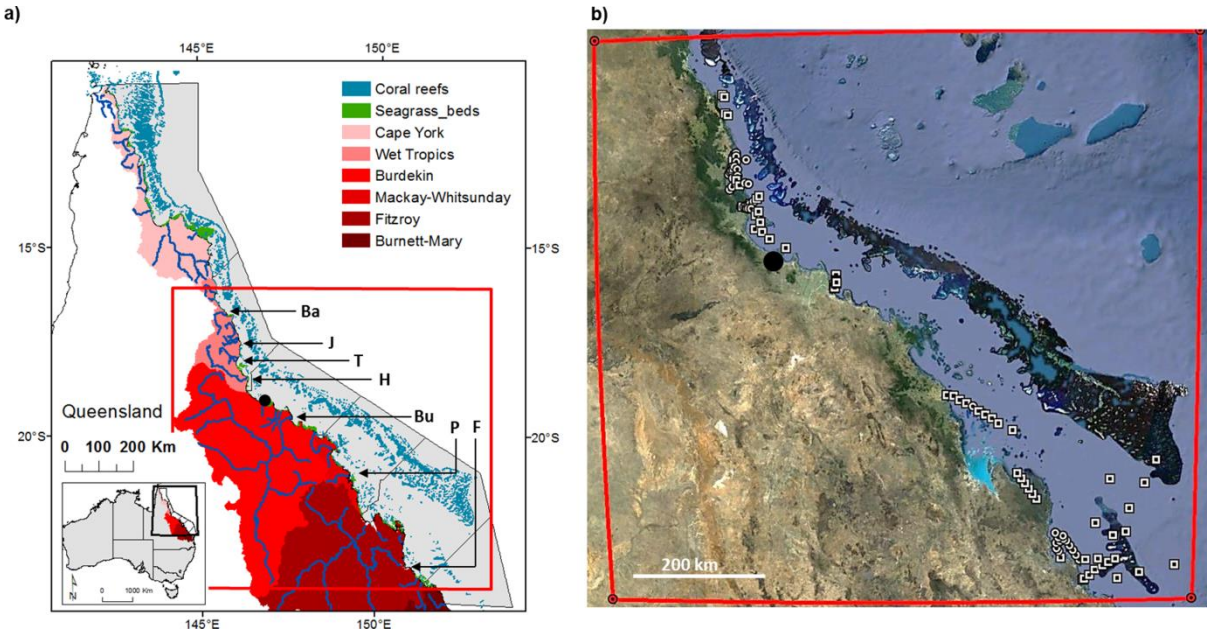

Fig. 1: Study area: Great Barrier Reef, Queensland, Australia. a) The Great Barrier Reef Marine Park (light grey, Queensland, Australia), major marine ecosystems (coral reefs and seagrass beds), catchments (red colour scale) and marine portions (delineated by dark grey liens) of the NRM regions and major rivers: Barron (Ba), Johnstone (J), Tully (T), Herbert (H), Burdekin (Bu), Pioneer (P), Fitzroy (F). b) Enlargement (red box) showing locations of WQ data measured during the 2010/11 and 2011/12 wet seasons. Sample locations are figured with white symbols: square symbols indicate locations sampled once and circles locations sampled regularly over the studied period. Large black dot stands for the Townsville city location.

Thirty major rivers drain into the GBR (Fig. 1a), all of which vary considerably in length, catchment area, and flow frequency and intensity. Rivers discharging into the GBR lagoon are the primary delivery mechanism for the input of land-based pollutants (i.e., sediments, nutrients and pesticides) into the GBR, though the actual distribution and movement of the individual pollutants varies considerably between the Wet (north of Townsville, Fig. 1a) and Dry Tropic rivers (Devlin et al.,

2011a). Rainfall and runoff rates are highly seasonal with over two thirds occurring during the summer wet season (December–April) in contrast to the dry season (May–November). Wet Tropic catchments, located between Townsville and Cooktown, have frequent storm and runoff events in generally short, steep catchments, and thus more direct and frequent linkages to coastal environments. In the Dry Tropic catchments, the major flow events may occur at intervals of years, with long lag times for the transport of material through these large catchments (Brodie et al., 2009).

The GBR catchment has been divided into six large areas defined as Natural Resource Management (NRM) regions (Fig. 1a), each defined by a set of land use/cover, biophysical and socio-economic characteristics. The Cape York region is largely undeveloped and is considered to have the least impact on GBR ecosystems from existing land based activities. In contrast, the Wet Tropics, Burdekin, Mackay-Whitsunday, Fitzroy and the Burnett-Mary regions are characterised by more extensive agricultural land uses including sugarcane, grazing, bananas and other horticulture, cropping, mining and urban development, and contribute to discharge of varying land-based pollutants to the GBR during the wet season. Occurrence of elevated concentrations of dissolved inorganic nitrogen (DIN) in coastal waters has been linked to fertilised agriculture (predominantly sugarcane) in the Wet Tropics and Mackay-Whitsunday regions, while high TSS concentrations are mainly linked to grazing activities in the Dry Tropics and in particular the Burdekin catchment (e.g., Brodie et al., 2008a, 2008b, 2012; Brodie and Waterhouse, 2009; Devlin and Brodie, 2005; Maughan and Brodie, 2009; Waterhouse et al., 2012).

2.2. Water quality data

In-situ data used in this study was collected as part of the GBR Marine Monitoring Program. The design of the flood monitoring program is detailed in Devlin et al. (2011c) with QC/QA procedures documented in GBRMPA (2012). Water samples to quantify chlorophyll-a, TSS and CDOM concentrations were collected from 0.5 m below the water surface and from multiple sites within the GBR plume waters extending from the Burnett-Mary (23°44'S) to Wet Tropics NRM regions (16°53'S), between November 2010 and March 2012 (Fig. 1b and Table 1).

Temperature, salinity and diffuse attenuation coefficient of photosynthetically active radiation (Kd(PAR)) were obtained from depth profiles using a CTD from Sea-Bird Electronics (SBE-19Plus). Salinity and temperature reported for the first 0.5 m of depth were calculated as the average of readings between 0.3 m and 0.7 m below the water surface. Kd(PAR) readings were calculated using the Lambert-Beer Equation (Dennison et al., 1993) (GBRMPA, 2012).

Sampling location was dependent on which rivers were flooding and the areal extent of the river plumes, but generally samples were collected in a series of transects heading out from the mouths of the rivers and towards the main direction of the river plume (Fig. 1b). Sampling frequency was dependent on the occurrence of flood events and access to the sampling sites.

2.3. Satellite data

Moderate Resolution Imaging Spectroradiometer (MODIS) Level 0 data (i.e., raw radiance counts) focusing on the summer wet season (December to April inclusive) were acquired from the NASA Ocean Colour website (http://oceancolor.gsfc.nasa.gov/) during three wet seasons (2010/11 to

2012/13). Satellite images were processed to L2 data (i.e., geophysical data) at 1 km resolution, using the SeaWiFS Data Analysis System (SeaDAS). SeaDAS is an internationally distributed image analysis package developed by NASA for processing, display, and analysis of satellite data (Baith et al., 2001). The program incorporates various operational bio-optical algorithms and has become the standard for MODIS ocean colour remote sensing processing (Qin et al., 2007). Different standard empirical and semi-empirical algorithms implemented in SeaDAS were tested for the retrieval of WQ data gradients as observed in-situ in the GBR river plume waters (Table 2).

Table 1: Number of WQ parameter (i.e., temperature, salinity, CDOM, TSS, chl-a, and Kd(PAR)) measured in-situ during the Wet Seasons 2010/11 and 2011/12. Data are grouped by month and numbers in brackets indicate days of the month the data were collected on. N is the number of sampling stations for each respective month.

Wet Season 2010-11	**N**	**Temp (◦C)**	**Sal**	**Kd(PAR) (m^{-1})**	**CDOM (m^{-1})**	**TSS (mg L^{-1})**	**chl-a (µg L^{-1})**
Nov 2010 *(22)*	13	13	13	0	13	13	13
Dec 2010 *(16, 28, 29, 30)*	26	22	24	20	26	20	44
Jan 2011 *(2, 4, 6, 10, 11, 17, 18, 19, 20, 25, 26)*	124	90	73	15	123	118	123
Feb 2011 *(7, 12, 13, 15, 17, 18, 20, 21, 22)*	96	89	89	0	95	82	96
March 2011 *(3, 25)*	31	31	31	0	31	31	30
April 2011 *(13, 14)*	14	7	14	0	14	0	14
Wet Season 2011-12	**N**	**Temp (◦C)**	**Sal**	**Kd(PAR) (m^{-1})**	**CDOM (m^{-1})**	**TSS (mg L^{-1})**	**chl-a (µg L^{-1})**
Sept 2011 *(9, 10)*	8	8	8	7	3	8	8
Nov 2011 *(28, 29)*	16	11	16	11	16	16	16
Dec 2011 *(19, 20)*	16	16	16	16	16	16	16
Jan 2012 *(5, 20, 21)*	29	29	29	28	29	29	29
Feb 2012 *(11, 13, 14)*	31	31	31	27	31	31	31
March *(5, 6, 8, 30, 31)*	60	35	61	53	56	60	60
Total	464	382	405	177	453	424	480

Chl-a concentrations were derived using the empirical Ocean Colour 3 (OC3; O'Reilly et al., 2000) and semi-analytical Garver-Siegel-Maritorena (GSM) (Garver and Siegel 1997; Maritorena et al., 2002) algorithms. In GBR coastal waters, the GSM algorithm was found to be more accurate than empirical band ratio approaches like OC3 (Qin et al. 2007) and has been used as proxy for chl-a concentration in river plume mapping (e.g., Devlin et al., 2012b). The OC3 algorithm was nevertheless described as successful to retrieve 0–10 µg L^{-1} chl-a concentrations (Odermatt et al., 2012) in optically complex water (i.e., case 2 waters: defined as waters influenced not just by phytoplankton and related particles, but also by other substances, that vary independently of phytoplankton, notably inorganic particles in suspension and yellow substances; Gordon and Morel, 1983; Morel, 1988; Morel and

Prieur, 1977). The absorption coefficient of detrital and coloured dissolved matters (CDOM+D) at a wavelength of 443 nm was retrieved using two semi-analytical algorithms implemented in SeaDAS: the Quasi-Analytical Algorithm (QAA, Lee et al., 2002) and the GSM algorithms. Both algorithms have been used as proxy to delineate GBR river plume extensions (Devlin et al., 2012b; Devlin and Schaffelke, 2009). The QAA algorithm was found more accurate than the GSM algorithm for the estimation of CDOM+D (Qin et al., 2007).

Table 2: Operational bio-optical algorithms tested for the RS retrieval of WQ data gradients as observed in-situ in the GBR river plume waters.

In situ WQ parameter	Satellite WQ proxy	algorithm	reference
chl-a (ug l^{-1})	chl-a-gsm (ug l^{-1})	Garver-Siegel-Maritorena (GSM)	Garver and Siegel 1997; Maritorena et al. 2002
	chl-a-oc3 (ug l^{-1})	Ocean Colour 3 (OC3)	O'Reilly et al., 1998, updated in O'Reilly et al., 2000
TSS (mg l^{-1})	nLw(645) (mW cm^{-2} um^{-1} sr^{-1})	SeaDAS standard processing	
	bbp(555)-qaa (555 nm, m^{-1})	Quasi-Analytical Algorithm (QAA)	QAA, Lee et al., 2002
CDOM (m^{-1})	CDOM+D-qaa (443nm, m^{-1})	Quasi-Analytical Algorithm (QAA)	QAA, Lee et al., 2002
	CDOM+D-gsm (443nm, m^{-1})	Garver-Siegel-Maritorena (GSM)	Garver and Siegel 1997; Maritorena et al. 2002
Kd(PAR)	Kd-Morel (490 nm, m^{-1})	Model of Morel	Morel, 1988; Morel et al., 2007
	Kd-Lee (488 nm, m^{-1})	model of Lee	Lee et al., 2005

The potential of MODIS data to retrieve suspended solids concentration gradients inside river plumes was evaluated using two TSS proxies: the backscattering particulate coefficient at 555 nm (bbp(555)-qaa) retrieved from the QAA algorithm and the normalized water leaving reflectance measured at 645 nm (nLw(645)). Both proxies have been used in the GBR for tracing particulate matters (Álvarez-Romero et al., 2013; Devlin et al., 2012b), while Álvarez-Romero et al. (2013) used the normalized water leaving reflectance measured at 667 nm. The potential of nLw(645) over nLw(667) was chosen based on recent studies (Doxaran et al., 2009; Lahet et al., 2010; Miller and Mckee, 2004; Ondrusek et al., 2012; Petus et al., 2010) showing a strong correlation between suspended sediment concentrations in turbid environments and reflectance values measured at 645 nm. This parameter has been indeed widely used as qualitative proxy for amounts of TSS in-water (e.g. Lahet et al., 2010) and has been integrated in empirical bio-optical algorithms to quantify the

concentrations of TSS (mg L^{-1}) or turbidity levels (NTU) (e.g., Doxaran et al., 2009; Miller and Mckee, 2004; Ondrusek et al., 2012; Petus et al., 2010).

Light attenuation through the water column can serve as a complementary WQ index (Weeks et al., 2012) for the discrimination of water types inside GBR river plumes. Two bio-optical models were selected and tested for the estimation of the light attenuation: the model of Morel (Morel, 1988; Morel et al., 2007) and the model of Lee (Lee et al., 2005) which simulate spectral diffuse attenuation at 490 nm (Kd-Morel) and 488 nm (kd-Lee), respectively. The first model is derived empirically through regression analyses using the relationship between Kd(490) and chl-a concentration, while the semi-analytical approach of Lee is based on radiative transfer models.A combined near-infrared (NIR) to short-wave infrared (SWIR) correction scheme (Wang and Shi, 2007), adapted to optically complex coastal waters, was applied to remove atmospheric contaminations. Processing SeaDAS filters, such as cloud and sun glint masks, were not used because they can result in large regions containing high sediment loads being masked. Clouds were post-masked using a 2.35% threshold on the Reyleigh corrected top of atmosphere radiance (Wang and Shi, 2006).

2.4. Water quality gradients inside river plumes and selection of L2 thresholds

Water types were mapped in this study following the studies of e.g., Devlin and Schaffelke (2009) and Devlin et al. (2010, 2012a, b). Based on in-situ WQ parameters, these studies described three distinct water types within GBR river plumes (from the inshore to the offshore boundary of river plumes) characterized by varying salinity levels, colour and WQ concentrations. Primary water type presents high turbidity, low salinity (0 to 10; Devlin et al., 2010), and very high values of CDOM and Total Suspended Sediment (TSS). Turbidity levels limit light penetration in Primary waters, inhibiting primary production and limiting chl-a concentration. Secondary water types are characterised by intermediate salinity, elevated CDOM concentrations, and reduced TSS due to sedimentation (Bainbridge et al., 2012). In this water type (middle salinity range: 10 to 25; Devlin et al., 2010), the phytoplankton growth is prompted by the increased light (due to lower TSS) and high nutrient availability (delivered by the river plume). Tertiary water type occupies the external region of the river plume. It exhibits no or low TSS associated with the river plume, and above-ambient concentrations of chl-a and CDOM. This water type can be described as being the transition between Secondary water and marine ambient water, presenting salinity lower than the former one (typically defined by salinity ≥ 35; e.g., Pinet, 2000).

Satellite-retrieved chl-a, CDOM+D, TSS (nLw(645), bbp(555)-qaa), and Kd(PAR) proxies were mapped over the study area for the wet seasons of 2010/11, 2011/2012, 2012/13 using SeaDAS and the algorithms presented on Table 2. Georeferenced MODIS L2 maps of the above-mentioned proxies were imported into Matlab software. Satellite-retrieved proxies corresponding geographically to the in-situ chl-a, CDOM, TSS and Kd(PAR) measurements were extracted using the nearest neighbour interpolation method implemented in Matlab; the value was taken from the MODIS L2 pixel that was closest to the geographical location of the in-situ WQ data, in this case 1 km was the maximum distance due to imagery resolution. In-situ and satellite WQ parameters inside river plumes were then grouped by salinity ranges following the Primary, Secondary and Tertiary water type classification as presented in Devlin and Schaffelke (2009) and Devlin et al. (2012b).

A discrimination power analysis on the 25th and 75th percentiles of the grouped WQ proxy values was conducted to select the best L2 product to discriminate the three water types. The discrimination power (i.e., the power to provide no or limited redundant information between the three water types) of each L2 product was judged according to the degree of inter-quartile overlap in box-plots (Barbour et al., 1996). We assigned a discrimination power of 3 if no overlap existed in the inter-quartile ranges, a power of 2 if inter-quartile ranges overlapped partly but did not reach either median, a value of 1 when there was an overlap of inter-quartile ranges but only one median was within the inter-quartile range of the other box, and 0 if both medians were within the inter-quartile range of the other box (Chen et al., 2014). Thresholds were determined by using the first quartile (Q1) of distributions of the selected Level 2 parameter for each water type**.** Daily maps of water types were produced for the three wet seasons using the selected L2 thresholds and the maps were then imported into a Geographic Information System (ArcGIS) for further post-processing.

2.5. Water type mapping

We overlaid the daily water type maps to assess (on a pixel-by-pixel basis) how frequently plumes and plume water types occurred. Frequency maps of exposure to each water type (Primary, Secondary and Tertiary) and for the presence or absence of plume waters were produced for each wet season as the number of days per wet season that a pixel value was retrieved as Primary, Secondary or Tertiary water type or classified as "plume" (i.e., retrieved as Primary or Secondary or Tertiary). The frequency of occurrence from each map produced was then grouped into classes (rare to very frequent) based on a "Natural Break (or Jenks)" classification. Jenks is a statistical procedure, embedded in ArcGIS as one of the basic classification schemes, that analyses the distribution of values in the data and finds the most evident breaks in it (i.e., the steep or marked breaks; Cromley and Mrozinski, 1997). The frequency classes were defined by applying the Jenks classification to the map of frequency of river plumes measured during the wet seasons 2012/2013, because this period presented the highest number of observations over the last 3 wet seasons. Frequency classes (number of days per wet season) were thus defined following Table 3.

Table 3: Frequency breaks used to scale all the frequency maps.

Frequency break (in days)	1 to 4	5 to 12	13 to 22	23 to 32	> 33
category	rare	infrequent	occasional	frequent	very frequent

2.6. Validation of the flood plume water type with true color MODIS data and comparison with in-situ water quality data

Two methods were applied to evaluate the supervised classification performance: (a) a visual comparison between MODIS plume water type maps and true colour images, and (b) a comparison between selected in-situ WQ parameters and the plume maps. For the visual comparison, two

distinct dates (04/01/2011 and 25/01/2011) presenting low coastal cloud cover, different flow conditions and different river plume waters were selected. For this comparison, a good supervised classification performance was indicated by a consistency on the colour gradients observed on the true color images and the three mapped water types. On the second method, the water type maps were compared against in-situ values of chl-a, TSS, CDOM, and Kd(PAR) acquired within ±2 h of the satellite over passes. The in-situ WQ parameters (i.e., chl-a, TSS, CDOM, and Kd(PAR), Table 1) were assigned to Primary, Secondary or Tertiary water type, based on their sampling time and location. For each water type, mean values ± 1 SD of chl-a, TSS, CDOM, and Kd(PAR) were calculated. A similar validation method was used by Devlin et al. (in press) to validate plume water type maps derived from classified true-colour MODIS Aqua images (Álvarez-Romero et al., 2013). In highly dynamic coastal waters, it is recommended to apply short time differences such as ±30 min (Doerffer, 2002) for in-situ/satellite data comparisons. In this study a longer time difference (±2 h) was selected to increase the sample size, as the in-situ data were not simultaneously collected to the satellite over passes.

3. Results

3.1. Water quality data

In total, 464 sites were sampled over 46 days, across five NRM regions, and during two wet seasons (2010/11 and 2011/2012). The concentrations of WQ parameters were variable within and among NRM regions (see Fig. A(a) in Supplementary material a), and across the two wet seasons (see Fig. A(b) in Supplementary material).

TSS concentrations throughout the flood events range from 0.4 to 92.0 mg l^{-1}. Chl-a concentrations and CDOM absorption coefficients were also variable, ranging from just below the detection limit to 5.0 µg l^{-1} and 3.6 m^{-1}, respectively. Of these 81% of chl-a (n = 373) and 86% of TSS (n = 364) measurements exceeded the annual WQ guidelines value set for the protection of GBR open coastal areas (i.e., 0.45µg l^{-1} and 2.0 mg l^{-1} for chl-a and TSS, respectively; (GBRMPA, 2010). Maximum salinity ranges were sampled in the Wet Tropics and Burdekin NRM (36.4 and 31.9, respectively). Kd(PAR) values were sporadically measured during the 2010/11 campaigns and systematically during the 2011/2012 campaigns (Table 1). Variation of Kd(PAR) over the sampling period strongly related to peaks in TSS, CDOM and chl-a concentrations (see Fig. A(b) in Supplementary material).

3.2. Water quality gradients inside river plumes and selection of L2 thresholds

Comparisons of in-situ and L2 satellite WQ gradients inside water types are presented in Fig. 2. In-situ WQ gradients (CDOM, TSS, and chl-a) plotted against salinity are consistent with the WQ gradients described by Devlin and Schaffelke (2009), but over a larger geographical area (the study of Devlin and Schaffelke was focused on the Tully coastal region).

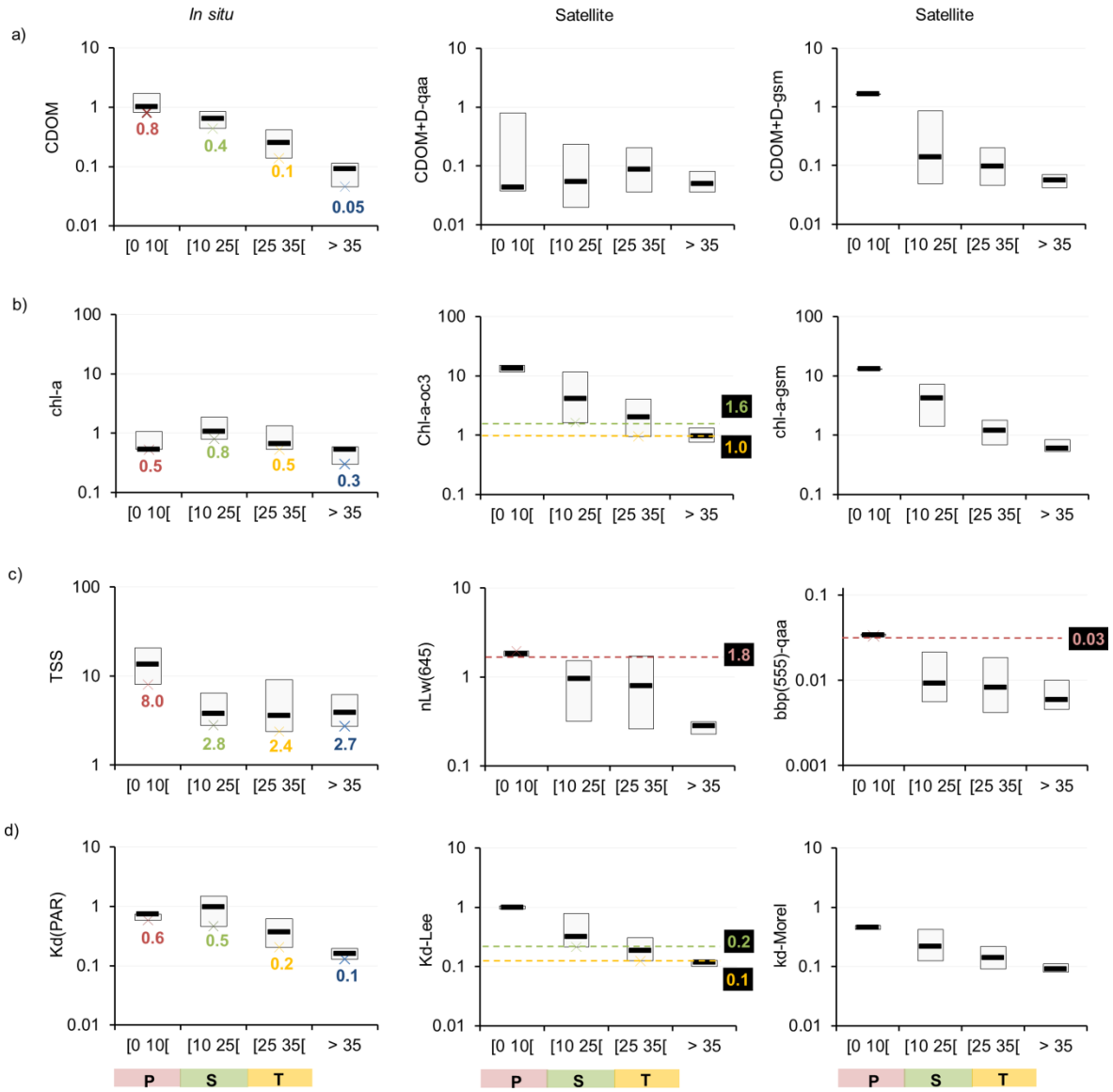

Fig. 2: Concentrations of the WQ parameters measured in-situ (left panel) and derived from satellite images (middle and right panels) within the GBR during flood events and grouped over salinity ranges (i.e., over the 3 water types, plus ambience marine water conditions). a) CDOM absorption measured in-situ (CDOM) and CDOM+D absorption estimated by QAA (CDOM+D-qaa) and GSM (CDOM+D-gsm) algorithms; b) chl-a concentrations measured in-situ (chl-a) and estimated by the OC3 (chl-a-oc3) and GSM algorithms (chl-a-gsm); c) TSS concentrations measured in-situ (TSS) and normalized water leaving reflectance (nLw(645)) and particulate backscattering coefficient estimated by the QAA algorithm (bbp(555)-qaa); and d) attenuation coefficient measured in-situ ((Kd(PAR)) and estimated by the Morel (Kd-Morel) and Lee algorithms (Kd-Lee). Box plot presents the median (dark black line), the third (Q3) and first (Q1) quartiles (rectangles) of values of WQ proxies over each water type. Q1 in-situ values are indicated under each box. Black labels indicate satellite thresholds (Q1 values) selected for delineating Primary, Secondary and Tertiary water types.

They confirm the existence of discernible water types inside river plumes characterised by specific salinity and WQ (CDOM, TSS, chl-a) concentrations (Fig. 2, left panel): (i) a Primary water type, which corresponds to the highly turbid river plume (salinity ranging between 0 to 10) and is characterized by high concentration of TSS and CDOM; (ii) a Secondary water type with intermediate salinity ranging between 10 and 25, characterised by lower TSS concentrations, though still significant content of the finer sediment fraction; and (iii) a Tertiary water type, defining the outer boundary of the river plume (salinity between 25 and 35), exhibiting reduced TSS, chl-a and CDOM compared to the other two water types, but where WQ data are still above those measured in ambient GBR marine waters (i.e., salinity ≥ 35).

While the absorption values of CDOM measured in-situ (Fig. 2a, left panel) show a good discrimination efficiency of water types (Table 4), satellite-derived CDOM+D values are redundant in the river plume salinity range (0 to 35; Fig. 2a, middle and right panels), particularly when using the QAA algorithm (Table 4). Decrease in chlorophyll concentrations from the Secondary to ambient marine waters (Fig. 2b, left panel) are well simulated by the OC3 and GSM algorithms (Fig. 2b, middle and right panels). However, both algorithms overestimate the pigment concentration in the Primary water type. These retrieval errors in inshore/estuarine waters are well documented and linked to the optical complexity of more coastal waters, where the overlapping and uncorrelated absorptions by dissolved organic matter and non-algal particles renders operational algorithms inaccurate for estimating chl-a concentration (e.g., Qin et al., 2007; Moses et al., 2009).

Table 4: Discrimination power of in-situ WQ data and corresponding satellite proxies: Marine, T: Tertiary, S: Secondary, P: Primary. A discrimination power of 3 indicate that no overlap exists in the inter-quartile ranges, a power of 2 that inter-quartile ranges overlap partly but did not reach either median, a value of 1 that inter-quartile ranges overlap but only one median is within the inter-quartile range of the other box, and 0 that both medians are within the inter-quartile range of the other box.

	WQ param/proxy	**M - T**	**T - S**	**S - P**
In-situ	CDOM	3	3	2
	chl-a	1	1	1
	TSS	0	0	3
	Kd(PAR)	3	2	1
Satellite	CDOM+D-qaa	1	0	0
	CDOM+D-gsm	1	0	3
	chl-a-oc3	***2***	***1***	3
	chl-a-gsm	2	2	3
	nLw(645)	0	0	**3**
	bbp(555)-qaa	1	0	**3**
	Kd-Lee	**1**	**2**	3
	Kd-Morel	1	1	2

Satellite-derived TSS proxies present high interquartile ranges for salinities > 10 and are redundant in Secondary and Tertiary water types (Fig.2c, middle and right panels and Table 4), similar to in-situ

TSS measurements (Fig. 2c, left panel and Table 4). This can be partially explained by the varying proportion of finer sediment fractions throughout the flood events. Finer sediment proportion can travel further with the river plume movement and drive the sediment concentrations in the outer part of the river plume (Bainbridge et al., 2012; Wolanski et al., 2008). Higher TSS concentrations measured in-situ in the Primary water type are linked to heavier particles before flocculation (Bainbridge et al. 2012; Brodie et al. 2010; Devlin and Brodie 2005). The settlement of these heavier particles in the water column is well represented by the satellite-derived TSS proxies, particularly bbp(555)-qaa (Fig. 2c, right panel and Table 4). Note that the difference (an order of magnitude) observed between bbp(555) and nLw(645) is in agreement with values published in literature. Oubelkheir et al. (2006) reported in-situ bbp(555) values ranging from 0.002 (offshore) to 2.806 (estuarine waters) in the Fitzroy Estuary and Keppel Bay system (GBR) and nLw(645) satellite values of 0.55 have been used by Lahet et al. (2010) to map the full extent of turbid river plumes in San Diego coastal waters (California). However, a restricted number (n = 1) of satellite-retrieved data available in the Primary plume limits a definitive validation of the bbp(555) and nLw(645) threshold proposed in this study.

Overall, in-situ light absorption values decrease with an increasing gradient of salinity (Fig. 2d). Median in-situ Kd(PAR) values (Fig. 2d, left panel) in the Secondary water type are higher (1 m-1) compared to those in Tertiary (0.4 m-1) and ambient marine waters (0.2 m-1). Median (0.7 and 1 m-1) and third quartile (0.6 and 0.5 m-1) values measured in-situ in the Primary and Secondary water types, respectively, are of the same order of magnitude. Good discrimination efficiency between attenuation coefficient data measured in Secondary and Tertiary water types are observed both in-situ (Fig. 2d, left panel) and using the satellite-derived data (Fig. 2d, middle and right panels), though best discrimination efficiency was obtained with the Kd-Lee algorithm (Table 4).

We selected thresholds to map water types (Table 5) based on the dominant characteristics of the GBR water types and satellite algorithms discrimination efficiency described in Table 4.

Table 5: L2 satellite thresholds selected.

	Primary (P)	**Secondary (S)**	**Tertiary (T)**
Characteristics	Turbidity maximum; Sediment-dominated.	Turbidity S < P; enhanced chl-a	Turbidity T < S ; CDOM, chl-a and Kd(PAR) > marine water Kd(PAR) < marine water
Discriminant Satellite thresholds (Q1)	nLw(645) ≥ 1.8 mW cm^{-2} um^{-1} sr^{-1} OR bbp(555)-qaa ≥ 0.03 m^{-1}	chl-a-oc3 ≥ 1.6 ug l^{-1} AND Kd-Lee ≥ 0.2 m^{-1}	chl-a-oc3 ≥ 1.0 ug l^{-1} OR Kd-Lee ≥ 0.1 m^{-1}

Tertiary and Secondary boundaries of river plumes (i.e., limits between the Tertiary and Marine water types and between Secondary and Tertiary water types) were delineated using a combination

of chl-a and/or light thresholds (Table 5 and Fig. B in Supplementary material). While the chl-a-gsm algorithm presents the best discrimination efficiency between Secondary and Tertiary water types (Table 4), we chose to use the OC3 algorithm (Table 5 and Fig. B in Supplementary material) because the GSM algorithm implemented in SeaDAS does not retrieve any chl-a value in areas of atmospheric perturbations (Salyuk et al., 2010). Furthermore, the OC3 algorithm was described as successful to retrieve relatively low chl-a concentrations (0–10 µg L-1) in optically complex water (Odermatt et al., 2012), values typically found in the GBR plume waters (Devlin et al., in press). High concentrations of TSS are the defining component of the Primary water type. As the high sediment concentrations measured in-situ in the Primary water type are well simulated by both the normalized water leaving reflectance and particulate backscattering proxies (Table 4), the Primary external boundary of the river plumes (i.e., the limit between the Primary and Secondary water types), was delineated using a combination of nlw(645) and bbp(555)-qaa thresholds (Table 5 and Fig. B in Supplementary material). Selected thresholds were thus successfully applied to sequentially map the Tertiary, Secondary and Primary water types, which were then overlaid to represent the full extent of the river plumes during the 2010/11 to 2012/13 wet seasons.

3.3. Validation of the method

3.3.1. Visual comparison between MODIS plume water type maps and true colour images

Enlargements of the Burdekin and Wet Tropics regions of water types (Primary, Secondary, and Tertiary) mapped over a 21-day period in January 2011 (04/01/2011 and 25/01/2011) are presented on Fig. 3a to demonstrate the supervised classification performance. They show that the main features of the river plumes observed in the true colour images are well captured by the selected thresholds (Fig. 3a). These two dates were selected to represent different flow conditions during the 2010/2011 wet season (Fig. 3b), and to include distinct river plume waters and low coastal cloud cover.

On the 4th and 25th of January, in the Burdekin region, brown/beige turbid waters, characteristic of sediment-dominated waters, were delineated as Primary water type. However, despite using a cloud mask method based on a SWIR reflectance threshold and developed for turbid water (Wang and Shi, 2006), the most turbid core of the river plume was misclassified as cloud (Fig. 3a) and could not be mapped as 'river plume' or specifically as Primary water type; a problem also noted by Álvarez-Romero et al. (2013). On the 4th and 25th of January, in the Wet Tropics, Primary waters were mapped close to the Barron, Johnston, Tully and Herbert river mouths and constrained close to the coast. Further offshore, the commonly observed northward movements of Secondary and Tertiary water types were well represented by the water type maps. These results show that the method developed in this study is suitable to categorise GBR river plume into broad types of surface waters representative of different WQ concentrations of dissolved and particulate matters and turbidity, and can be useful to map the movement patterns of river plumes.

Nearly all of the GBR rivers experienced a high degree of flooding over the 2010-11 wet season (Fig. 3b) due to the very strong 'La Nina' beginning in mid-2010 and three cyclones (Tasha in late December 2010, Anthony in late January 2011 and Yasi in early February 2011) that crossed the North Queensland coast over a period of three months (e.g., Devlin et al., 2012b). River plumes mapped in January are characterized by different orientations and shapes as well as different colours, underlying the high spatio-temporal variability and changing WQ properties (Fig. 3a) existing

in GBR River plumes. In both the Burdekin River and Wet Tropics regions, river plumes were interconnected and covered the whole inshore regions. On the 4th of January, the Tertiary plume reached coral reefs in the Wet Tropics.

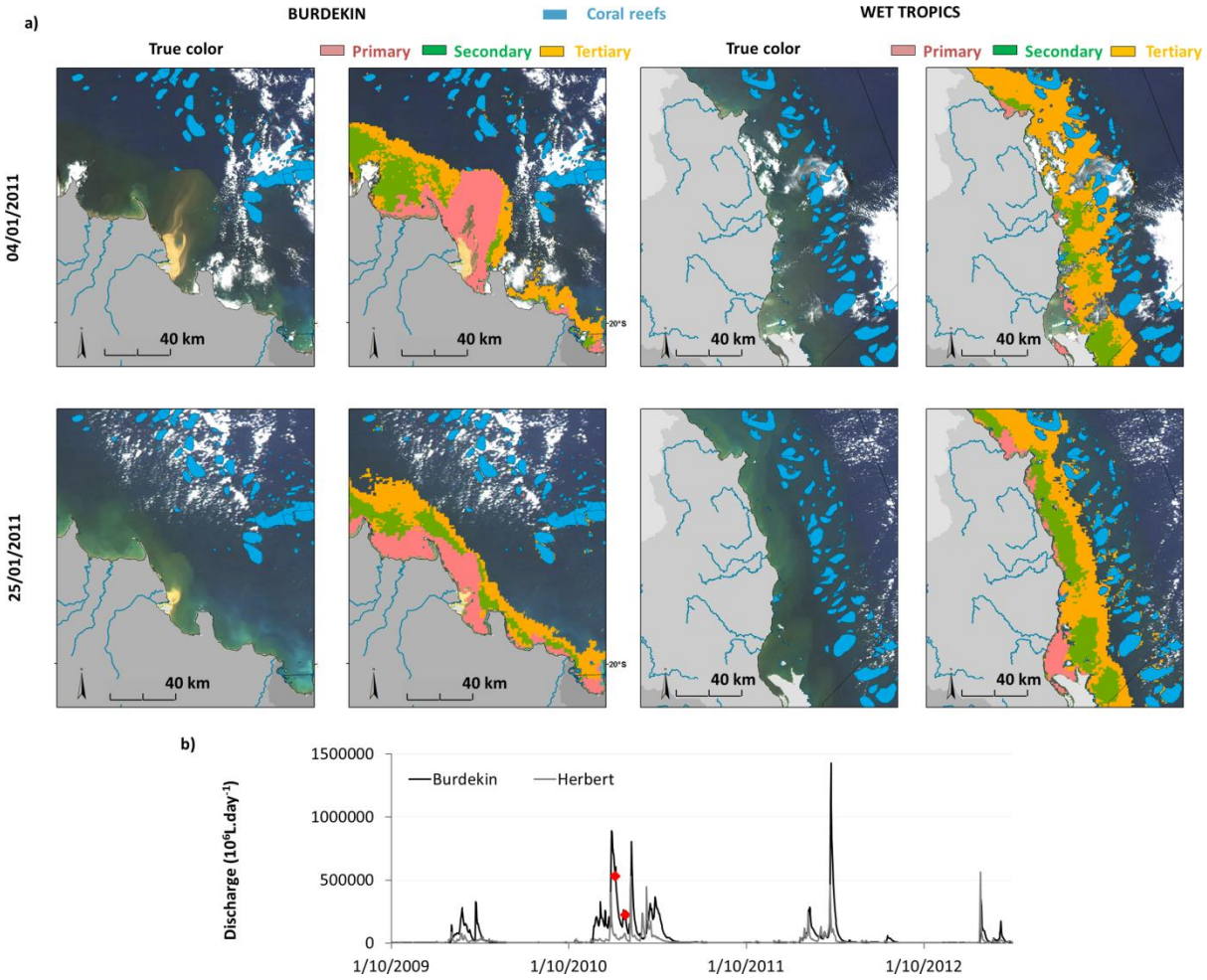

Fig. 3: a) Enlargement of MODIS maps over Burdekin and Wet Tropics regions illustrating the temporal and spatial dynamics of GBR river plumes: true color composite and water types mapped the 04th and 25th of January 2011 using the selected satellite thresholds. Areas misclassified as cloud are encircled in white; b) Daily flow measurements for Burdekin River and Herbert River (Wet Tropics) over the 2011-12 wet season. The 04th and 25th of January 2011 are identified by red dots.

3.3.2.Comparison with in-situ water quality data

In-situ water quality concentrations (chl-a, TSS, CDOM, KdPAR) were assigned to a plume water type class (i.e., Primary, or Secondary, or Tertiary; see Fig. C in supplementary material). Water quality concentrations across the three plume water types, with the exception of TSS, are comparable with our current understanding of water quality gradients (as described by e.g. Devlin and Schaffelke, 2009; Devlin et al., 2012a and Devlin et al., in press; see section 2.4). The Kd(PAR) and CDOM values reduce through the three flood plume water types from 0.67 m^{-1} and 0.35 m^{-1}(Primary) to 0.32 m^{-1}

and 0.22 m^{-1} (Tertiary), respectively. The chl-a concentration are lower in the initial turbid primary water type (0.75µg L^{-1}) and increase through the secondary water type (0.96 µg L^{-1}) as sedimentation increases and nutrient concentrations stay elevated. TSS concentration reduced from the Secondary (10 mg L^{-1}) to the Tertiary (5 m L^{-1}) water type. The low TSS concentrations in the Primary water type, as compared to e.g. Devlin et al. (in press) could be attributed to the limited number of TSS data points available within ±2 h time difference between in-situ collection and the satellite over passes in the primary water type data (only 2 TSS measurements). Despite this limitation, these concentrations gradients (see Fig. C in supplementary material) support the validity of the supervised classification method applied in this study.

3.4. Annual maps of river plume frequency

Over the three mapped wet seasons (2010/11 to 2012/13), river plumes (including the Primary, Secondary and Tertiary water types) extended from Cape York to the south of the Fitzroy River (Fig. 4).

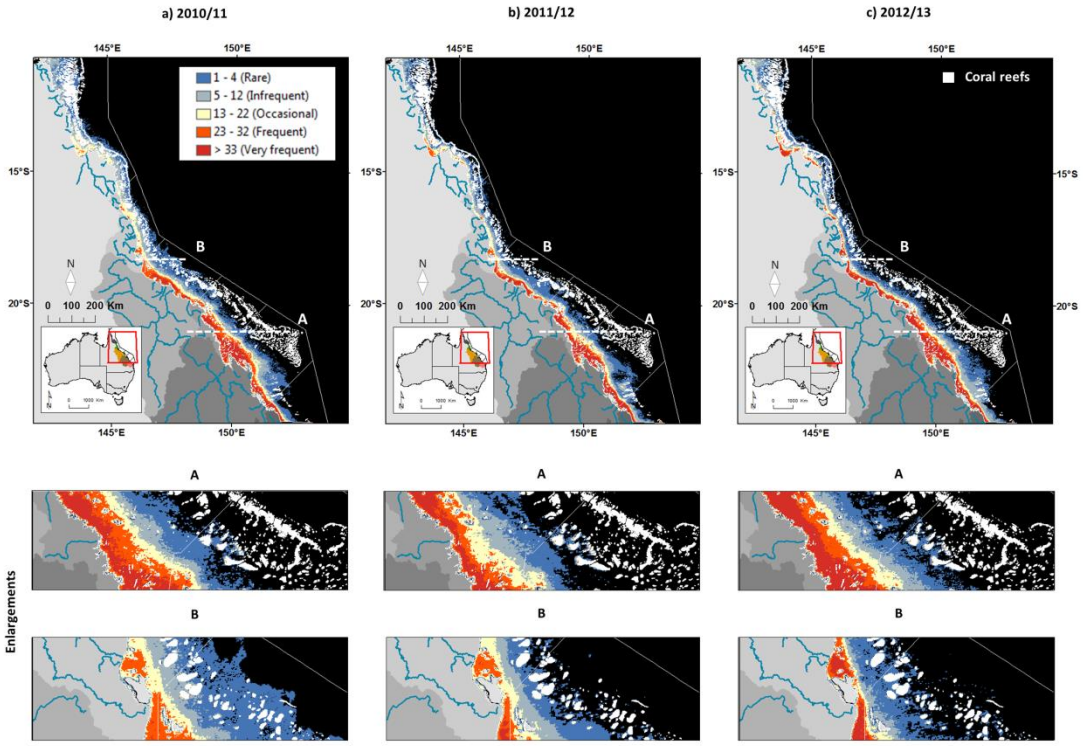

Fig. 4: Frequency of occurrence (in days per wet season) of the GBR river plumes mapped during the wet seasons of a) 2010/11, b) 2011/12 and c) 2012/13 and enlargements over A): the Pioneer and, B) the Tully and Herbert rivers. Frequency (in days per wet season) was calculated using the full extent river plume maps (i.e., summed water type maps derived using the selected satellite thresholds). Note the relatively larger river plumes mapped for the 2010/2011 wet season.

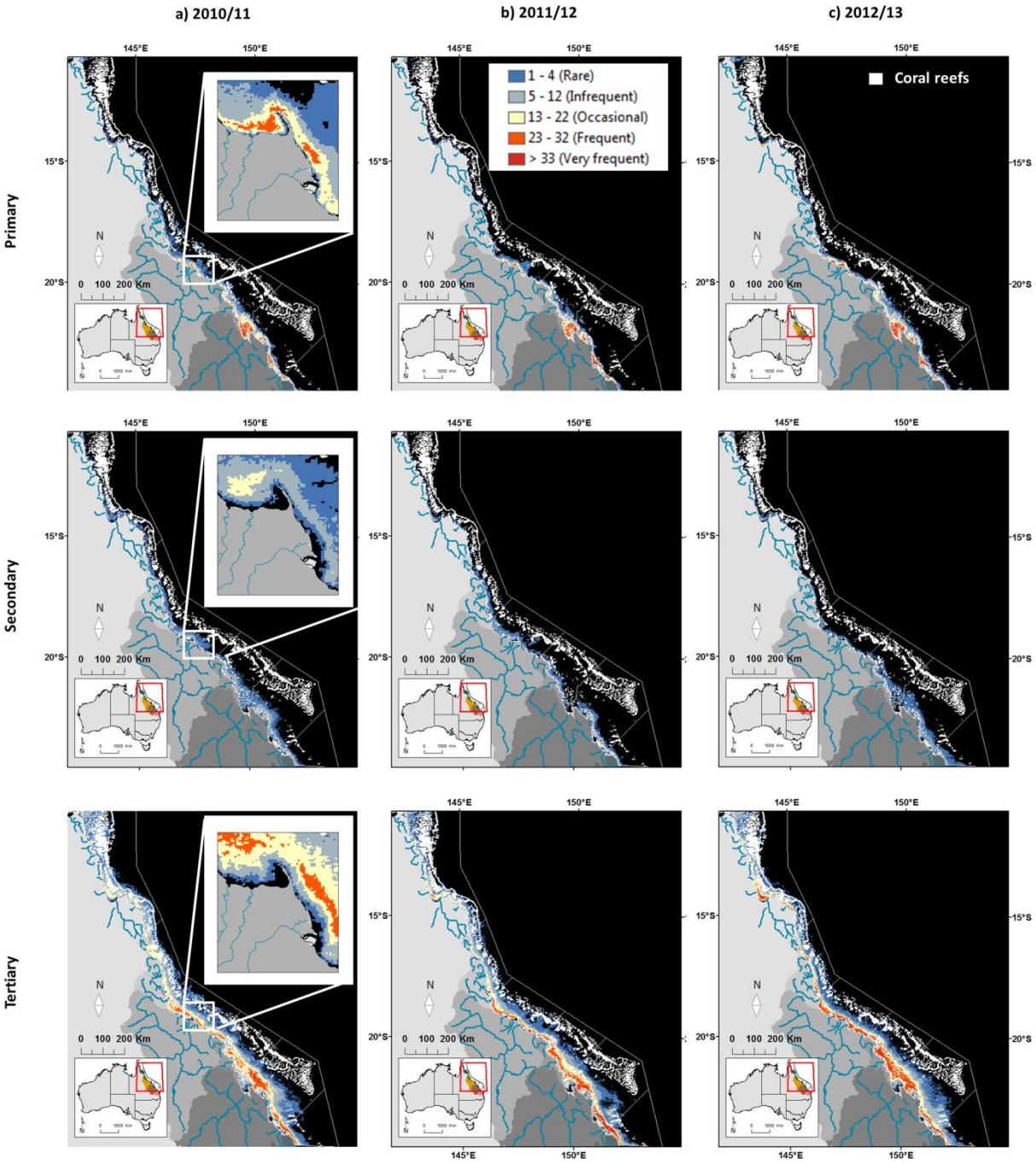

Fig. 5: Frequency of occurrence (in days per wet season) of GBR water types measured during the wet seasons of a) 2011, b) 2012 and c) 2013.

Inshore zones within 20-30 km were areas the most exposed (occasionally to very frequently, as defined in Fig. 4) to river plumes, though river plumes were larger during the extreme flood events of the wet season 2010/11 than during the 2011/12 and 2012/2013 wet seasons (see enlargement over the Pioneer, Tully and Herbert rivers).Composition of the river plumes differed significantly from the inshore to offshore areas (Fig. 5). Primary water type occurred near to the coast and occasionally to frequently in a coastal band of up to 40 km in the vicinity or major rivers (Fig. 5, Primary). High phytoplankton biomass (measured by high chl-a concentrations used to describe the Secondary water type) occurred more frequently at some distance from the coast, as observed on

the enlargement of the Burdekin river (Fig. 5, Secondary). The Secondary water type occurred parallel to the coast and reached distance offshore of up to 100 km. These observations are in agreement with preliminary results obtained by Devlin et al. (2012a). During the 3 studied years, Tertiary waters located in the most outer core of the river plume (Fig. 5, Tertiary) were the most likely to reach the outer GBR reefs.

As observed with the full extent maps (Fig. 4), the greatest extent of Primary, Secondary and Tertiary water types occurred during the 2010/11 wet season (Fig. 5a, b and c). The highest frequency of Primary water was found around the Burdekin river, where high TSS concentrations in river flow and coastal waters have been linked to grazing activities (e.g., Brodie and Waterhouse, 2009; Devlin and Brodie, 2005; Maughan and Brodie, 2009). High frequency of Primary water type was also mapped in Shoalwater Bay, north of the Fitzroy River mouth. In this shallow coastal zone, observed turbid water masses are more likely to be caused by sediment resuspended by strong tidal currents (Kleypas, 1996), than turbid river plumes from the Fitzroy river mouth. This underlines one of the limitations of the method: other surface water masses with similar optical and color characteristics can be confounded with the different water types. Similar problems were highlighted by Álvarez-Romero et al. (2013).

4. Discussion

The protection of the GBR ecosystems from increasing pollution is recognised as one of the critical issues for management of the World Heritage Area (Brodie and Waterhouse, 2012; Haynes et al 2001). Mapping the location, frequency and composition of river plumes provides key information to help assess the risk of ecological impacts from degraded water quality (river plume risk). This study describes a method that maps wet season WQ gradient patterns across GBR regions that are consistent for each selected WQ parameter and that can be easily reproduced using satellite-derived data. This study confirmed the existence of three main water types within the GBR river plumes (Devlin et al., 2012; Devlin and Schaffelke, 2009). The relatively simple approach proposed to delineate these water types and to map river plumes, through the assignment of thresholds against readily available bio-optical algorithms, facilitates the processing of large numbers of images. It thus permitted the assessment of spatial-temporal variability across large regions and multi-annual (in this case, three wet seasons) periods.

It should be emphasized that the major purpose of our study was to develop a process which utilised the best of optimal, and readily available bio-optical algorithms in SeaDAS, rather than to produce new regional bio-optical algorithms. This study was orientated to produce cost effective methods, using freely available MODIS images and methods that can be reproduced by non-remote-sensing specialists with minimum training in RS/GIS methods, and to provide useful information for managers. Our method is readily applicable for studies of GBR on large temporal scales (10 years of MODIS images are archived and available on the NASA ocean colour website) and potentially to other regions, given that the thresholds are regionally adjusted following the process proposed here.

4.1. Use of quantitative thresholds in defining water types

Ocean colour satellite data, like MODIS images, offer frequent (daily) and synoptic (whole GBR scale) pictures of GBR coastal environments and thus can help with identification and mapping of GBR river plumes. Two families of supervised classification methods based on MODIS data have been recently investigated to map marine areas exposed to freshwater and different water types as well as the transport of pollutant inside the GBR river plumes. The first family of analysis (hereinafter 'True colour method') is based on classification of spectrally enhanced quasi-true colour MODIS images and has been used to classify 'river plume' and 'non-river plume' areas in the GBR (Álvarez-Romero et al., 2013; Bainbridge et al., 2012). This method exploits the differences in colour between the turbid river plumes and the marine ambient water, and between respective water types inside the river plumes (Álvarez-Romero et al., 2013). The second family of analysis (hereinafter 'L2 threshold method'), which this study describes, uses threshold values applied to atmospherically corrected Level-2 products derived from satellite images to delineate river plume boundaries and surface water types inside river plumes (e.g., Dzwonkowski and Yan, 2005; Saldias et al., 2012; Schroeder et al. 2012).

Both methods rely on the same principle: gradients of WQ existing in river plumes (from the estuary mouth to the edge of the river plume) modify the optical signature of the water (related to the concentration of TSS, chl-a, CDOM), which in turn change the colour of the water. Both methods present advantages and disadvantages: the true colour method offers a simple and objective method by clustering the information contained in MODIS true-colour composites (Red–Green–Blue bands), but relies on non-atmospherically corrected data, and usually the spectral signature used to classify images does not incorporate potential temporal and spatial variability. The L2 threshold method assume fixed WQ value/level/concentration thresholds and thus also ignores potential temporal and spatial variability, but does account for atmospheric correction. In addition, this method offers valuable quantitative information, such as the concentration of CDOM, TSS, chl-a, or Kd(PAR) values that are not directly available through the clustering of the true-colour composites. This quantitative information is essential to evaluate the concentration/level/load of stressors discharged through river plumes during the wet season and to assess potential ecological impacts.

Exact bio-optical algorithms to retrieve WQ proxies in optically complex estuarine and inshore waters are still in development. Recent progress has been made to develop regional algorithms for the GBR region (Brando et al., 2012; Schroeder et al., 2012), that provide better retrieval in optically complex coastal waters. MODIS images processed by these regional algorithms will be instrumental in more accurate mapping of river plume waters. Nevertheless, the method presented in this study based on WQ gradients in order to map broad water bodies (i.e., Primary, Secondary or Tertiary waters types) does not have a strong dependence on single quantitative pixel retrieval through the mapping of general trends of satellite WQ. The L2 threshold method developed in this study does not require accurate retrieval of satellite WQ proxies above the L2 thresholds defined (Table 5) as such MODIS pixel would be classified as river plume water anyway.

4.2. Towards the production of risk maps for the GBR ecosystems

The risk of a particular ecosystem (e.g., in the GBR, seagrass meadows or coral reefs) to be affected by a particular stressor (in this case pollutants associated with river plumes) can be assessed by evaluating:

(i) The likelihood of the risk, i.e., how likely a particular stressor is to happen. This can be estimated by calculating the frequency of occurrence of river plumes or specific water types;
(ii) The magnitude of the risk, i.e., in river plume risk analysis, the intensity quantified as concentration, level or load of pollutant discharge through the river plume, in this case described by the different water types; and
(iii) The ecological consequences of the risk, i.e., the extent of the ecological impact for a particular ecosystem given a combination of magnitude and likelihood of occurrence of the stressor.

Information on the factors that influence the likelihood and magnitude of occurrence of river plumes water types and the associated water quality characteristics can help direct on-ground water quality management by prioritising action on the activities that contribute to regional water quality measures (e.g., US EPA, 1998 and Fig. D in Supplementary material).

Collection of information at the most appropriate temporal and spatial scales is difficult using only traditional biogeochemical methods owing to the constraints of direct sampling (Devlin and Schaffelke, 2009). Remote sensing technologies provide the synoptic window and repetition necessary to investigate changes in WQ conditions over time and, in combination with in-situ data, provide an opportunity to investigate the risk of reduced coastal WQ from the river discharge.

Measuring the magnitude of the river plume risk to coral reefs and seagrass beds is challenging because different stressors are combined in surface plume waters. Devlin et al. (2012b) underscored the need to develop risk models that incorporate the cumulative effects of pollutants. Secchi Disk Depth (SDD) can be estimated from in-situ Kd(PAR) measurement using the approximate relation of Holmes (1970): Kd(PAR) = 1.44 SDD. Using this relation, Kd(PAR) levels (measured by the Q1 value) in Primary, Secondary and Tertiary water types (Fig. 2; Kd ≥ 0.6, Kd ≥ 0.5, Kd ≥ 0.2, respectively) are equivalent to SDD levels (SDD ≤ 2.4 m, SDD ≤ 2.9 m, SDD ≤ 7.2 m) all under the minimum trigger value of 10 m set for the protection and maintenance of marine species and ecosystem health of the GBR open coastal areas by the Great Barrier Reef Marine Park authority (GBRMPA 2010). Elevated levels of turbidity, which limit light penetration, and reduce the amount of light available for seagrass photosynthesis, are described as the primary cause of seagrass loss (Mckenzie et al. 2012; Collier et al. 2012). Coral biodiversity also declines as a function of increasing turbidity throughout the GBR (De'ath and Fabricius 2010) and reef development ceases at depths where light is below 6-8% of surface irradiance (Cooper et al. 2007; Titlyanov and Latypov 1991). Thus the magnitude of the risk for these ecosystems from reduced water clarity will increase from the Tertiary/edge waters to the Primary/inshore core of river plumes.

Furthermore, more than 90% of the land-sourced nutrients enter the GBR lagoon during high flow periods (Brodie et al., 2012; Mitchell et al., 2005). A linear decrease of DIN concentrations across river plumes (from the coast to offshore i.e., from Primary to Tertiary water types) have been described by Álvarez-Romero et al. (2013). Photosystem II inhibiting herbicides (PSII herbicides) at elevated concentrations have also been traced during the wet season in river plumes from catchments to the GBR lagoon (Davis et al., 2008). It was demonstrated by Kennedy et al. (2012) and Lewis et al. (2009a) that the concentrations of PSII herbicides on the GBR typically exhibit a linear decline across the salinity gradient (i.e., from Primary to Tertiary water types). As a first approximation, it can thus be assumed that the magnitude of the river plume risk for the GBR seagrass beds and coral reefs from combined WQ stressors will increase from the Tertiary waters to

the Primary core of river plumes. Classification of surface waters into Primary, Secondary, and Tertiary water types can thus provide a mechanism to cluster cumulative WQ stressors into three (ecologically relevant) broad categories of risk magnitude.

At the multi-annual scale, understanding the changes in the frequency of occurrence of these surface water types are relevant to a better understanding of the likelihood of river plumes and the different categories of risk magnitude. Producing annual maps of frequency of Primary, Secondary, and Tertiary water types in the GBR lagoon thus can summarise the combined likelihood and magnitude of the river plume risk over a defined time period. This can also help to identify movements and dispersal abilities of water types and, in combination with ecosystem maps, can serve as the basis to assess potential ecological consequences imposed by different levels of likelihood and magnitude of river plume risk. Fig. 6b presents an example of river plume risk maps produced for the three studied wet seasons (2010/11 to 2012/13). These maps have been produced using a simple risk matrix (Fig. 6a) assuming that potential risk level for GBR ecosystems can be ranked in four qualitative categories (very high, high, medium and low) determined by the combination of the magnitude and the likelihood of the river plume risk (modified from Castillo et al., 2012).

Our satellite observations (Fig. 4, Fig. 5 and Fig. 6) are in agreement with theoretical models (Geyer et al., 2004; Wiseman Jr and Garvine, 1995), previous physical oceanographic studies (Wolanski and Jones 1981; Wolanski and van Senden 1983) and modelling studies (King et al., 1997) of river plumes in the GBR, and suggest that river plumes are constrained close to the coast by Coriolis forces and the prevailing wind regime, limiting impacts on the more offshore ecosystems. However under offshore wind conditions, river plumes can be deflected seaward and occasionally reach the mid and outer-shelf of the GBR reef (Brodie et al., 1997; Fig. 4 and Fig. 5). Mid and outer-shelf of the GBR reef are nevertheless more likely to be affected by the Tertiary water type (i.e., lower risk category) levels than the Primary turbid core of the river plumes (Fig. 5).

The mapping of exposure and water types does also depend on the frequency and availability of the MODIS images. In this study, the maximum number of observations (on a pixel basis) was 66 days (Fig. 4 and Fig. 5) i.e., about 40% of the annual wet season days. Furthermore, more river plumes were mapped in the Dry Tropics than in the Wet Tropics NRM regions, particularly during the wet season 2010/2011, related to extended flow periods. MODIS time-series used in this study are restricted by cloud cover which prevents ocean colour observations and the description of the plume through optical satellites images. These observations underline the climatic limitations of our satellite-based methodology. Similar limitations nevertheless apply when using in-situ measurements as shipboard surveys and sampling data quality are highly dependent of the wind and sea conditions (Nezlin et al., 2007). It means that, whatever the monitoring system employed, it is difficult to describe the plume during maximum flood events and thus the maximum plume extent may be underestimated. Nevertheless, satellite images combined with in-situ WQ data offer the most extensive spatial and temporal coverage available to monitor river plumes.

a)

Likelihood \ Magnitude	Tertiary	Secondary	Primary
rare	low	low	medium
infrequent	low	medium	medium
occasional	medium	medium	high
frequent	medium	high	high
very frequent	high	high	very high

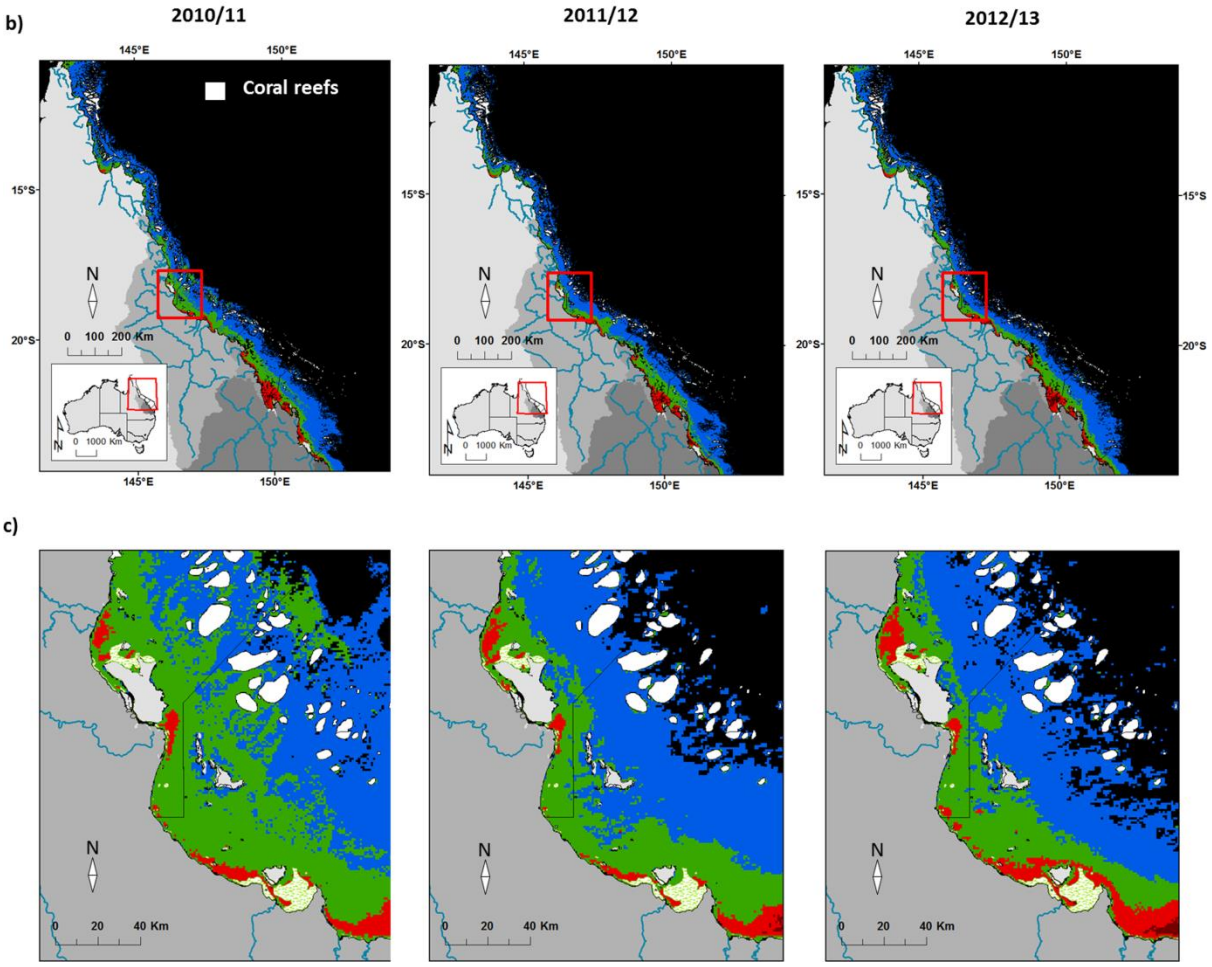

Fig. 6: a) Qualitative evaluation of likelihood and magnitude of river plumes (modified from Castillo et al., 2012); b) 2010/11, 2011/12 and 2012/13 river plume risk maps and c) zooms on the Tully River to Ross Rivers.

Finally, analysis of the magnitude and likelihood of the risk from the remote sensing data must be accompanied by sound knowledge of the regional ecosystems to produce river plume risk assessment of reef and seagrass ecosystems. Ecological consequences of the risk will primarily be a function of the presence/absence of GBR ecosystems subjected to different occurrence and magnitude of risk. A risk does not exist unless (i) the stressor has the inherent ability to cause one or more adverse effects, and (ii) it co-occurs or comes into contact with an ecological component (i.e., organisms, populations, communities, or ecosystems; US EPA, 1998) susceptible to the stressor. In

the GBR, many seagrass meadows occur in coastal and estuarine areas close to the source of sediments (Fig. 1a and Fig. 6c), and are thus more likely to be impacted by Primary water type than ecosystems located more offshore such as mid-shelf and outer-shelf coral reefs. Community characteristics such as the sensitivity and resilience of particular seagrass or coral communities (e.g., associated with their natural levels of exposure to pollutants) are additional parameters that must be considered when defining the ecological consequences of the risk. Indeed, different species assemblages will respond differently to the same exposure (i.e., same likelihood × magnitude of risk) to river plumes. The consequence of the exposure of species to a range of WQ conditions is complicated by the influence of multiple stressors and additional external influences including weather and climate conditions, and consequences are mostly unknown at a regional or species level (Brodie et al., 2013).

Further work is also required to improve our understanding of the river plume risk, particularly around the duration of river plume occurrence or maximum concentration/level/load of stressor discharged in extreme weather events in order to further define the magnitude of risk. This information, i.e., the number of continuous days or weeks this ecosystem was in contact with river plumes or particular water types, is available through the processing of daily MODIS data. In-situ WQ data are regularly acquired in the GBR lagoon and will help to further validate the threshold values proposed in this study over a longer time period. Future in-situ sampling should mainly focus on sampling WQ proxies in the Primary water type of river plumes (salinity < 10), as a significant number of data are missing in the highly turbid plume waters. This study looked for overall and thus, simplified WQ gradient patterns across GBR regions. Regional studies relating the concentrations of WQ data to salinity profiles should be additionally examined to investigate the transport of pollutants and gradients of change within GBR river plumes at the NRM scale. Finally, the method developed in this study should be applied on a larger temporal scales (10 years of MODIS images are available) to provide significant information for policy makers and catchment managers on river plume risk for reef and seagrass ecosystems.

Conclusion

This study presents a method to classify river plume waters into three surface water types by using a supervised classification applied on MODIS L2 data. Comparison of WQ gradients measured in-situ during river flood events and WQ estimated from MODIS images showed good agreement and thus were used to determine relevant satellite proxies and threshold values that can be used for the delineation of the water types. Using the selected thresholds, water type maps were produced over three wet seasons. These maps can help to define the likelihood and magnitude of the risk of reduced coastal WQ associated with the river discharge (river plume risk) for coastal GBR marine ecosystems. Examining remote-sensing information in the context of marine and coastal ecological risk assessments is useful as satellite methodologies give synoptic and repeatable measurements of relative WQ changes. Remote sensing data help to understand scales (temporal and spatial) of the risk that affect the ecosystems at large synoptic scale (i.e., GBR-scale) and help define over what geographical and temporal scales the effect should be monitored and managed.

Acknowledgement

Authors gratefully acknowledge support from the Centre for Tropical Water and Aquatic Ecosystem Research (TropWATER). We also would like to thank the Great Barrier Reef Marine Park Authority and Department of Sustainability, Environment, Water, Population and Communities (DSEWPaC) for funding support and the Reef Plan Marine Monitoring Program which was the main source of in-situ data for this study. JGAR acknowledges the support of the Australian Research Council and Consejo Nacional de Ciencia y Tecnología (CONACyT).

Supplementary material

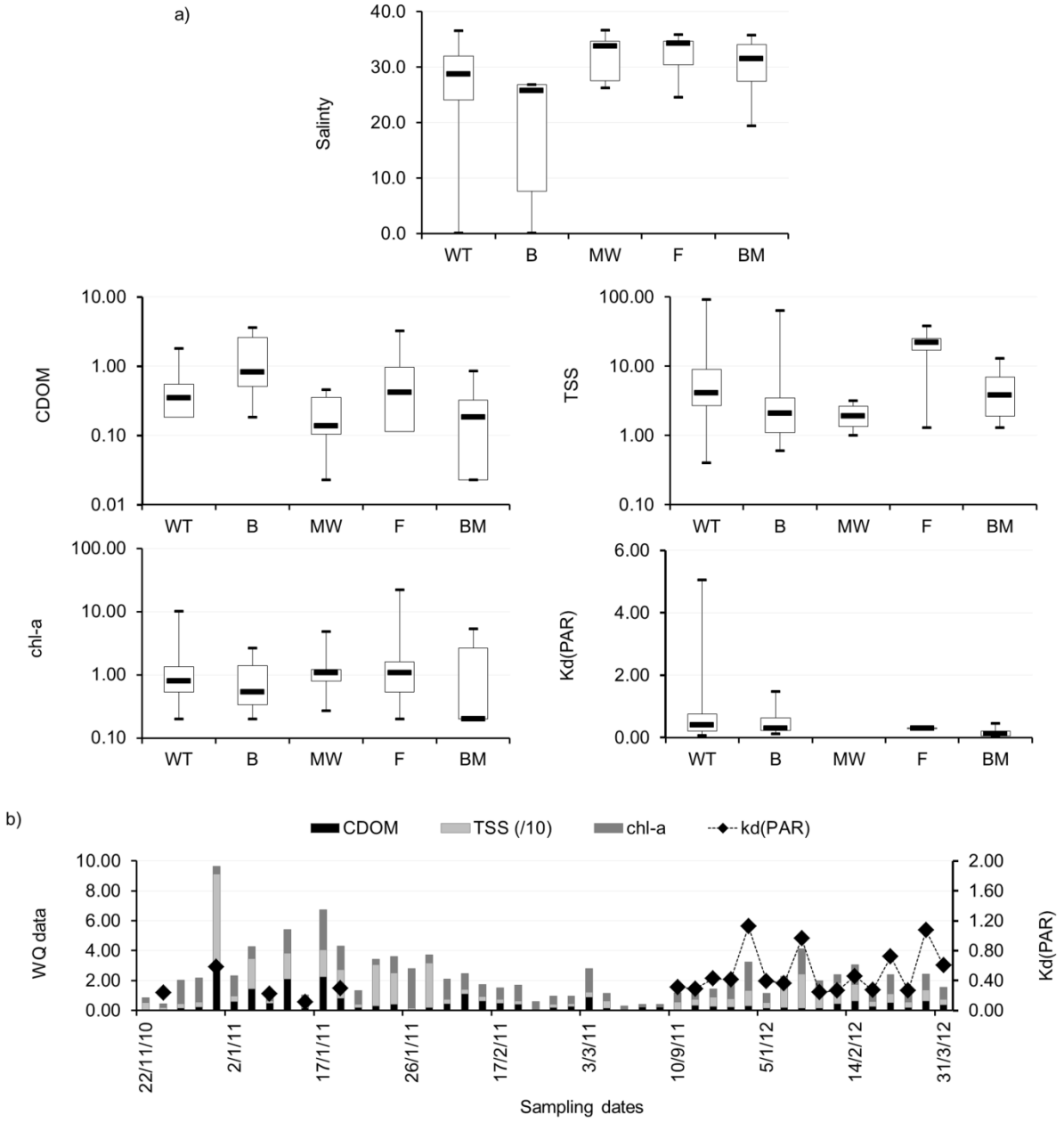

Fig. A (previous page): Range of salinity, WQ data (CDOM, in m-1; chl-a in µg L-1 and TSS in mg L-1 and Kd(PAR) in m-1) measured in-situ in five NRM regions in the GBR (Wet Tropics: WT; Burdekin: B; Mackay-Whitsundays: MW; Fitzroy: F, and Burnet-Mary: BM). (a) Box plot presents the median (dark black line), the first (Q1) and third (Q3) quartiles (rectangle), and minimum and maximum values of the WQ data over each NMR (vertical lines). (b) Variation of WQ parameters (CDOM, chl-a and TSS and Kd(PAR), median values per sample date) measured over the 2010-2011 and 2011-2012 wet seasons.

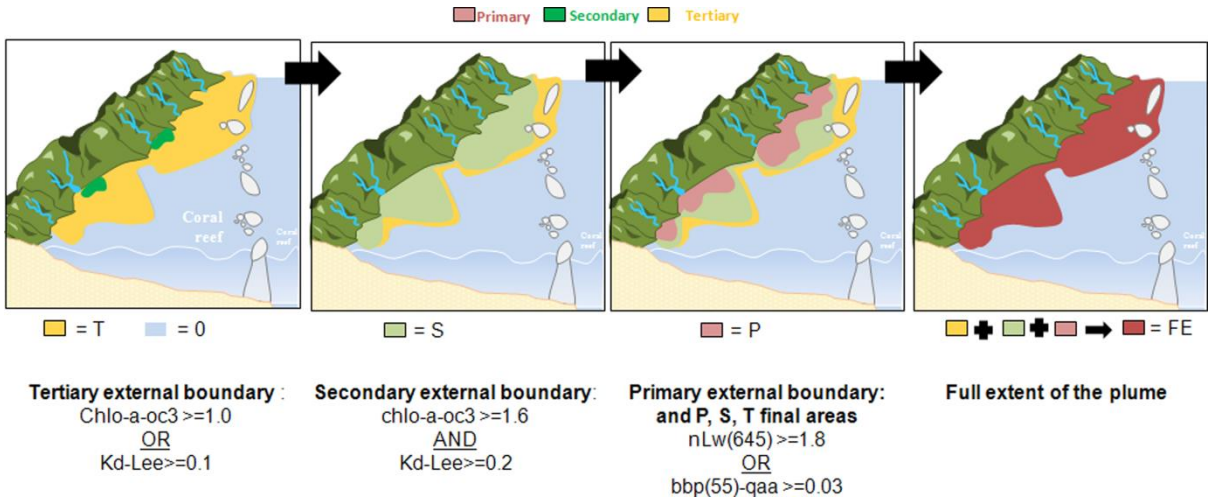

Fig. B: method used to delineate Primary (P), Secondary (S), and Tertiary (T) water types and the full extent (FE) of GBR river plume waters.

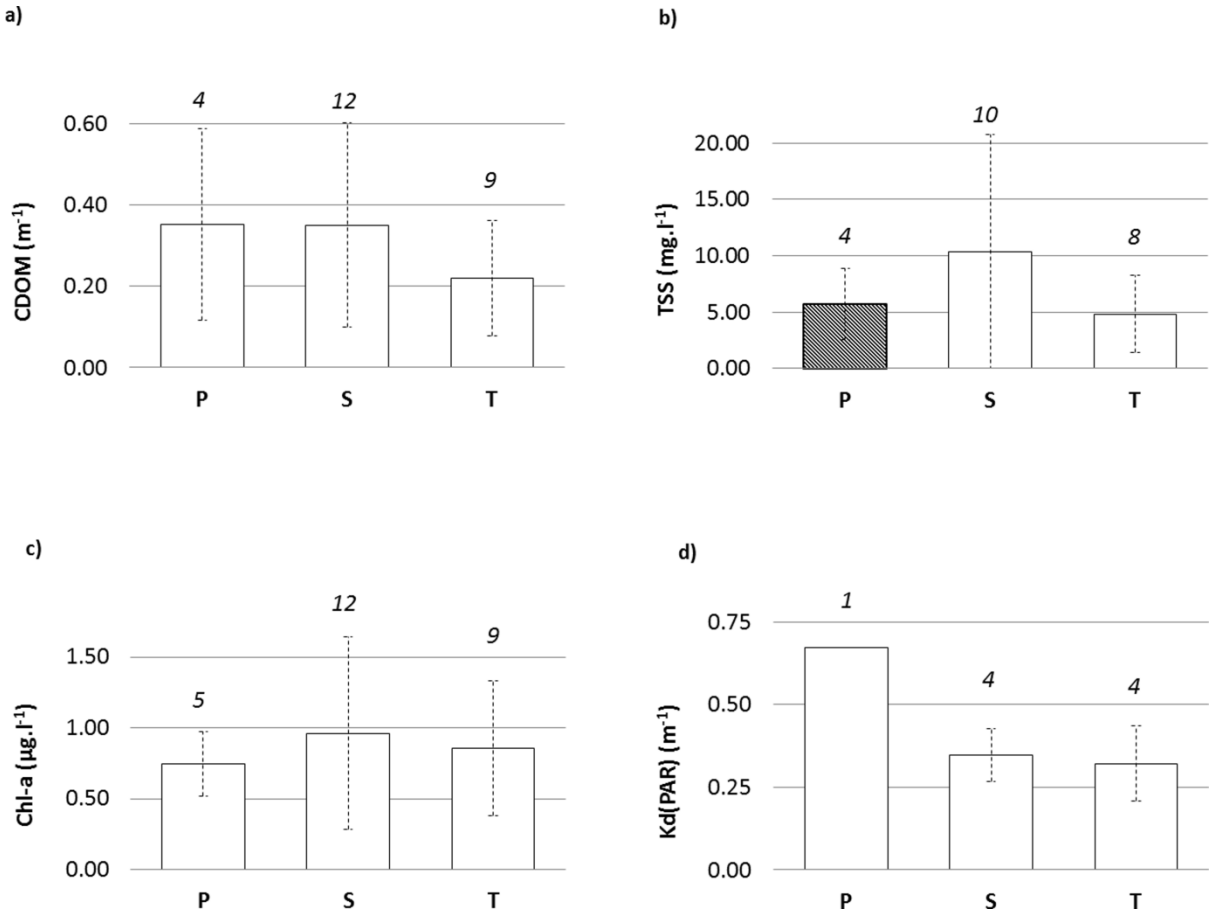

Fig. C: Mean concentrations of in-situ water quality measurements within each plume type. Water quality data assigned to plume water when the difference between in-situ collection and the satellite over passes is within ±2 h. Number of data is indicated in italic.

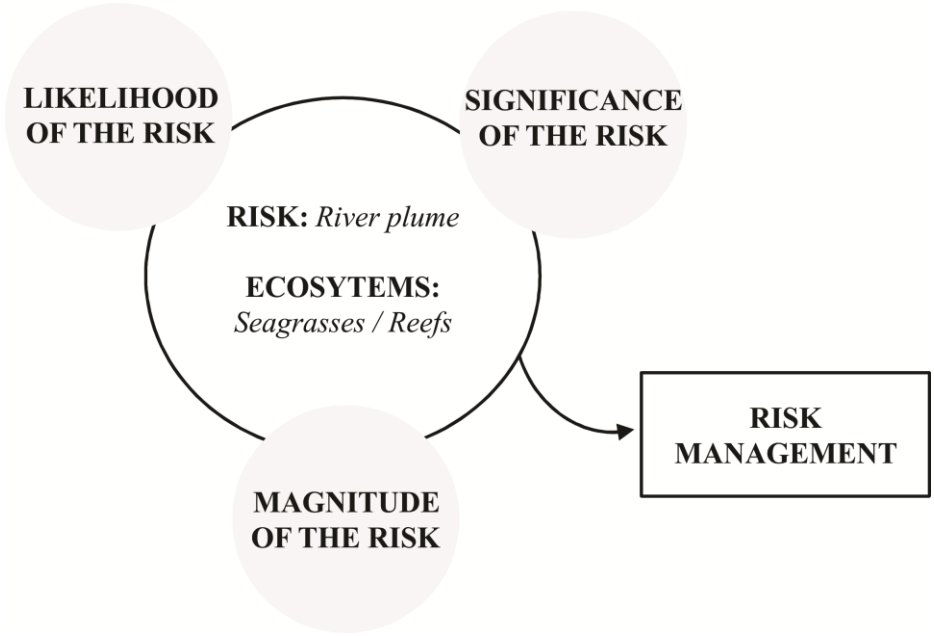

Fig. D: GBR ecosystem risk assessment scheme.

Bibliography

Álvarez-Romero, J.G., Devlin, M., Teixeira da Silva, E., Petus, C., Ban, N.C., Pressey, R.L., Kool, J., Roberts, J., Cerdeira, S., Wenger, A.S., Brodie, J., 2013. A novel approach to model exposure of coastal-marine ecosystems to riverine flood plumes based on remote sensing techniques. J. Environ. Manage. 119, 194-207.

Bainbridge, Z., Wolanski, E., Álvarez-Romero, J.G., Lewis, S., Brodie, J., 2012. Fine sediment and nutrient dynamics related to particle size and floc formation in a Burdekin River flood plume, Australia. Mar. Pollut. Bull. 65, 236-248.

Baith, K., Lindsay, R., Fu, G., McClain, C.R., 2001. SeaDAS, a data analysis system for ocean color satellite sensors. Eos Trans. Am. Geophys. Union 82, pp. 202.

Barbour, M.T., Gerritsen, J., Griffith, G.E., Frydenborg, R., McCarron, E., White, S., Bastian, M.L., 1996. A framework for biological criteria for Florida streams using benthic macroinvertebrates. J. N. Am. Benthol. Soc. 15, 185–211.

Brodie, J.E., Steven, A., Baer, M., 1997. The extent of river plumes associated with cyclone Sadie rainfall. In: A.D.L. Steven (Ed.), Cyclone Sadie Flood Plumes in the Great Barrier Reef Lagoon: Composition and Consequences, Workshop Series No. 22, Great Barrier Reef Marine Park Authority, Townsville, Australia.

Brodie, J., Binney, J., Fabricius, K., Gordon, I., Hoegh-Guldberg, O., Hunter, H., O'Reagain, P., Pearson, R., Quirk, M., Thorburn, P., Waterhouse, J., Webster, I. Wilkinson, S., 2008a. Scientific Consensus Statement on Water Quality in the Great Barrier Reef. The State of Queensland (Department of the Premier and Cabinet) Brisbane, Australia.

Brodie, J., Binney, J., Fabricius, K., Gordon, I., Hoegh-Guldberg, O., Hunter, H., O'Reagain, P., Pearson, R., Quirk, M., Thorburn, P., Waterhouse, J., Webster, I. Wilkinson, S., 2008b. Synthesis of evidence to support the Scientific Consensus Statement on Water Quality in the Great Barrier Reef. The State of Queensland (Department of the Premier and Cabinet) Brisbane, Australia.

Brodie, J.E., Waterhouse, J., Lewis, S.E., Bainbridge, Z.T., Johnson, J., 2009. Current loads of priority pollutants discharged from Great Barrier Reef Catchments to the Great Barrier Reef. ACTFR Report 09/02. Australian Centre for Tropical Freshwater Research, Townsville, Australia.

Brodie, J.E., Waterhouse, J., 2009. Assessment of the relative risk of impacts of broad-scale agriculture on the Great Barrier Reef and priorities for investment under the Reef Protection Package. Stage 1 Report: April 2009. ACTFR Report 09/17. Australian Centre for Tropical Freshwater Research, Townsville, Australia.

Brodie, J., Schroeder, T., Rohde, K., Faithful, J., Masters, B., Dekker, A., Brando, V.,

Maughan, M., 2010. Dispersal of suspended sediments and nutrients in the Great Barrier Reef lagoon during river discharge events: Conclusions from satellite remote sensing and concurrent flood plume sampling. Mar. Freshwater Res. 61, 651-664.

Brodie, J., Waterhouse, J., Maynard, J., Bennett, J., Furnas, M., Devlin, M., Lewis, S., Collier, C., Schaffelke, B., Fabricius, K., Petus, C., da Silva, E., Zeh, D., Randall, L., Brando, V., McKenzie, L., O'Brien, D., Smith, R., Warne, M.S.J., Brinkman, R., Tonin, H., Bainbridge, Z., Bartley, R., Negri, A., Turner, R.D.R., Davis, A., Bentley, C., Mueller, J., Álvarez-Romero, J.G., Henry, N., Waters, D., Yorkston, H., Tracey, D., 2013. Assessment of the relative risk of water quality to ecosystems of the Great Barrier Reef. A report to the Department of the Environment and Heritage Protection, Queensland Government, Brisbane. TropWATER Report 13/28, Townsville, Australia.

Brodie, J., Waterhouse, J., 2012. A critical review of environmental management of the 'not so Great' Barrier Reef. Estuar. Coast Shelf S.104-105, 1-22.

Brodie, J.E., Kroon, F.J., Schaffelke, B., Wolanski, E.C., Lewis, S.E., Devlin, M.J., Bohnet, I.C., Bainbridge, Z.T., Waterhouse, J., Davis, A.M., 2012. Terrestrial pollutant runoff to the Great Barrier Reef: An update of issues, priorities and management responses. Mar. Pollut. Bull. 65, 81-100.

Castillo, M.E., Baldwin E.M., Casarin R.S., Vanegas, G.P., Juarez M.A., 2012. Characterization of Risks in Coastal Zones: A Review. Clean – Soil, Air, Water 40, 894–905.

Chen, K., Hughes, R.M., Xu, S., Zhang, J., Cai, D., Wang, B., 2014. Evaluating performance of macroinvertebrate-based adjusted and unadjusted multi-metric indices (MMI) using multi-season and multi-year samples. Ecol. Indic. 36, 142-151.

Clarke, G.L., Ewing, G.C., Lorenzen, C.J., 1970. Spectra of backscattered light from sea obtained from aircraft as a measure of chlorophyll concentration. Science 16, 19–21.

Cooper, T.F., Uthicke, S., Humphrey, C., Fabricius, K.E., 2007. Gradients in water column nutrients, sediment parameters, irradiance and coral reef development in the Whitsunday Region, central Great Barrier Reef. Estuar. Coast Shelf S. 74, 458-470.

Cromley, R.G., Mrozinski, R. D., 1997. An evaluation of classification schemes based on the statistical versus the spatial structure properties of geographic distributions in chloropleth mapping. American Congress on Surveying and Mapping Technical papers, 5, 76-85.

Davis, A., Lewis, S., Bainbridge, Z., Brodie, J., Shannon, E., 2008. Pesticide residues in waterways of the Lower Burdekin Region: challenges in ecotoxicological interpretation of monitoring data. Australas. J. Ecotox. 14, 89-108.

De'ath, G., Fabricius K., 2010. Water quality as a regional driver of coral biodiversity and macroalgae on the Great Barrier Reef. Ecol. Appl. 20, 840-850.

Devlin, M., Brodie, J., 2005. Terrestrial discharge into the Great Barrier Reef Lagoon: nutrient behaviour in coastal waters. Mar. Pollut. Bull. 51, 9-22.

Devlin, M., Schaffelke, B., 2009. Spatial extent of riverine flood plumes and exposure of marine ecosystems in the Tully coastal region, Great Barrier Reef. Mar. Freshwater Res. 60, 1109-1122.

Devlin, M., Barry, J., Mills, D.K., Gowen, R.J., Foden, J., Sivyer, D., Greenwood, N., Pearce, D., Tett, P., 2009. Estimating the diffuse attenuation coefficient from optically active constituents in UK marine waters. Estuar. Coast Shelf. S. 82, 73-83.

Devlin, M., Waterhouse, J., McKinna, L., Lewis, S., 2010. Terrestrial runoff in the Great Barrier Reef. Marine Monitoring Program (3.7.2b). Tully and Burdekin case studies. Reef Rescue Marine Monitoring Program (MMP) Publications, 87 pp.

Devlin, M., Schroeder, T., McKinna, L., Brodie, J., Brando, V., Dekker, A., 2011a. Monitoring and mapping of flood plumes in the Great Barrier Reef based on In situ and Remote Sensing observations. In: Chang, N. (Ed.), Environmental Remote Sensing and Systems Analysis, Taylor and Frances Group – the CRC Press, Australia, pp.147–190.

Devlin, M., Harkness, P., McKinna, L., Waterhouse, J., 2011b. Mapping the surface exposure of terrestrial pollutants in the Great Barrier Reef. Report to the Great Barrier Reef Marine Park Authority, August 2010. ACTFR report 10/12. Australian Centre for Tropical Freshwater Research, Townsville, Australia.

Devlin, M., Wenger, A.S., Waterhouse, J., Álvarez-Romero, J.G., Abbot, B., da Silva, E.T., 2011c. Reef Rescue Marine Monitoring Program: Flood Plume Monitoring Annual Report 2010-11. Incorporating results from the Extreme Weather Response Program flood plume monitoring. ACTFR report 02/12. Australian Centre for Tropical Freshwater Research, Townsville, Australia.

Devlin, M.J., McKinna, L.W., Álvarez-Romero, J.G., Petus, C., Abott, B., Harkness, P., Brodie, J., 2012a. Mapping the pollutants in surface riverine flood plume waters in the Great Barrier Reef, Australia. Mar. Pollut. Bull. 65, 224-35.

Devlin, M.J., Brodie, J., Wenger, A.S., McKinna, L.W., da Silva, E.T., Álvarez-Romero, J.G.,Waterhouse, J., McKenzie, L., 2012b. Extreme weather conditions in the Great Barrier Reef: Drivers of change? Proceedings of the 12th International Coral Reef Symposium, Cairns, Australia, 9-13 July 2012.

Devlin, M.J., da Silva, E.T., Petus, C., Wenger, A.S., Zeh, D., Tracey, D., Álvarez-Romero, J., Brodie, J., in press. Combining in-situ water quality and remotely sensed data across spatial and temporal scales to measure wet season chlorophyll-a variability: Great Barrier Reef lagoon (Queensland, Australia). Ecological Processes.

Doron, M., Bélanger, S., Doxaran, D., Babin, M., 2011. Spectral variations in the near-infrared ocean reflectance. Remote Sens. Environ. 115, 1617-1631.

Doxaran D., Froidefond, J.M., Castaing, P., Babin, M., 2009. Dynamics of the turbidity maximum zone in a macrotidal estuary (the Gironde, France): Observations from field and MODIS satellite data. Estuar. Coast Shelf. S. 81, 321-332.

Dzwonkowski, B., Yan, X.H., 2005. Tracking of a Chesapeake Bay estuarine outflow plume with satellite-based ocean color data. Cont. Shelf Res. 25, 1942-1958.

Fabricius, K.E., 2011. Factors determining the resilience of coral reefs to eutrophication: a review and conceptual model. In: Dubinsky, Z., Stambler, N. (Eds.), Coral Reefs: An Ecosystem in Transition. Springer Science + Business Media B.V., pp. 493-506.

Garver, S.A., Siegel, D.A., 1997. Inherent optical property inversion of ocean color spectra and its biogeochemical interpretation: I. Time series from the Sargasso Sea. J. Geophys. Res. 18, 607-18,625.

Geyer, W.R., Hill, P.S., Kineke, G.C., 2004. The transport, transformation and dispersal of sediment by buoyant coastal flows. Cont. Shelf Res. 24, 927-949.

Gordon, H., Morel, A., 1983. Remote Assessment of Ocean Colour for Interpretation of Satellite Visible Imagery: A Review. Lecture Notes on Coastal and Estuarine Studies, Vol. 4, Springer Verlag, New York, 114 pp.

Gordon, H.R., Wang, M., 1994. Retrieval of water-leaving radiance and aerosol optical thickness over the oceans with SeaWiFS: A preliminary algorithm. Appl. Optics 33, 443-452.

Great Barrier Reef Marine Park Authority, 2010. Water Quality Guidelines for the Great Barrier Reef Marine Park. Great Barrier Reef Marine Park Authority, Revised edition 2010, Townsville, Australia, 100 pp.

Great Barrier Reef Marine Park Authority, 2012. Reef Rescue Marine Monitoring Program: Quality Assurance/Quality Control Methods and Procedures. Great Barrier Reef Marine Park Authority Townsville, Australia, 104 pp.

Haynes, D., Brodie, J., Christie, C., Devlin, M., Michalek-Wagner, K., Morris, S., Ramsay, M., Storrie, J., Waterhouse, J., Yorkston, H., 2001. Great Barrier Reef water quality: Current issues, Great Barrier Reef Marine Park Authority, Townsville, Australia, 90 pp.

Horner-Devine, A.R., Jay, D.A., Orton, P.M., Spahn, E.Y., 2009. A conceptual model of the strongly tidal Columbia River plume. J. Marine Syst. 78, 460-475.

IOCCG, 2008. Why ocean colour? The societal benefits of ocean-colour technology. International Ocean-Colour Coordinating Group, Science, 141 pp.

Jeffrey, S.W., Humphrey, G.W., 1975. New spectrophotometric equations for determining chlorophylls a, b, c and c2 in higher plants, algae and natural phytoplankton. Biochemie und Physiologie der Pflanzen 167, 191-198.

Kennedy, K., Schroeder, T., Shaw, M., Haynes, D., Lewis, S., Bentley, C., Paxman, C., Carter, S., Brando V. E., Bartkow, M., Hearn, L., Jochen, F., Mueller, J. F., 2012. Long term monitoring of photosystem II herbicides – Correlation with remotely sensed freshwater extent to monitor changes in the quality of water entering the Great Barrier Reef, Australia. Mar. Pollut. Bull. 65, 292-305.

King, B., Spagnol, S., Wolanski, E. Done, T., 1997. Modeling the mighty Burdekin River in flood. Fifth International Conference on Coastal and Estuarine Modeling, Washington D.C., 22-24 October 1997.

Kleypas, J.A., 1996. Coral reef development under naturally turbid conditions: fringing reefs near Broad Sound, Australia. Coral Reefs 15, 153-167.

Kroon, F.J., Kuhnert, P., Henderson, B., Wilkinson, S., Henderson, A., Brodie, J., Turner, R., 2012. River loads of suspended solids, nitrogen, phosphorus and herbicides delivered to the Great Barrier Reef lagoon. Mar. Pollut. Bull. 65, 167-181.

Lahet, F., Stramski, D., 2010. MODIS imagery of turbid plumes in San Diego coastal waters during rainstorm events. Remote Sens. Environ. 114, 332-344.

Lee, Z.P., Carder, K.L., Arnone, R.A., 2002. Deriving inherent optical properties from water color: a multiband quasi-analytical algorithm for optically deep waters. Appl. optics 41, 5755-5772.

Lee, Z.P., Du, K.P., Arnone, R.A., 2005. A Model for the diffuse attenuation coefficient of downwelling irradiance. J. Geophys. Res. 110, C02016, doi: 10.1029/2004JC002275.

Maritorena, S., Siegel, D.A., Peterson, A.R., 2002. Optimization of a semianalytical ocean color model for global-scale applications, Appl. Optics 41, 2705- 2714.

Matthews, M.W., 2012. A current review of empirical procedures of remote sensing in inland and near-coastal transitional waters. Int. J. Remote Sens. 32, 6855-6899.

Maughan, M., Brodie, J., 2009. Reef exposure to river-borne contaminants: a spatial model. Mar. Freshwater Res. 60, 1132-1140.

McKenzie, L., Unsworth, R., 2011. Surviving the flood; How long can seagrass “hold its breath”?,in McKenzie, L., Yoshida, R. L., Unsworth R., (Eds). Seagrass-Watch News. Seagrass-Watch HQ.

Miller, R.L., McKee, B.A., 2004. Using MODIS Terra 250 m imagery to map concentrations of total suspended matter in coastal waters. Remote Sens. Environ. 93, 259-266.

Molleri, G.S.F., de M. Novo, E.M.L., Kampel, M., 2010. Space-time variability of the Amazon River plume based on satellite ocean color. Cont. Shelf Res. 30, 342-352.

Morel, A., Prieur, L., 1977. Analysis of variations in ocean color. Limnol. Oceanogr. 22, 709-722.

Morel, A., 1988. Optical modelling of the upper ocean in relation to its biogenous matter content (case 1 waters). J. Geophys. Res. 93, 10,749-10,768.

Morel, A., Huot, Y., Gentili, B., Werdell, P.J., Hooker, S.B., Franz, B.A., 2007. Examining the consistency of products derived from various ocean color sensors in open ocean (Case 1) waters in the perspective of a multi-sensor approach. Remote Sens. Environ. 111, 69- 88.

Moses, W.J., Gitelson, A.A., Berdnikov, S, Povazhnyy, V., 2009. Estimation of chlorophyll-a concentration in case II waters using MODIS and MERIS data - successes and challenges. Environ. Res. Lett. 4, 045005, 1-8.

Nezlin, N.P., DiGiacomo, P.M., Diehl, D.W., Jones, B.H., Johnson, S.C., Mengel, M.J., Reifel, K.M., Warrick, J.A., Wang, M., 2008. Stormwater plume detection by MODIS imagery in the southern California coastal ocean. Estuar. Coast Shelf. S. 80, 141-152.

Nezlin, N.P., DiGiacomo, P.M., Jones, B.H., Reifel, K.M., Warrick, J.A., Johnson, S.C., Mengel, M.J., 2007. MODIS imagery as a tool for synoptic water quality assessments in the southern California coastal ocean. Proc. SPIE 6680, Coastal Ocean Remote Sensing, September 28, 2007, 66800T.

Odermatt, D., Gitelson, A., Brando, V.E., Schaepman, M., 2012. Review of constituent retrieval in optically deep and complex waters from satellite imagery. Remote Sens. Environ.118, 116-126.

Ondrusek, M., Stengel, E., Kinkade, C.S., Vogel, R.L., Keegstra, P., Hunter, C., Kim, C., 2012. The development of a new optical total suspended matter algorithm for the Chesapeake Bay. Remote Sens. Environ.119, 243-254.

O'Reilly, J., S. Maritorena, B. G. Mitchell, D. A. Siegel, K. L. Carder,M. Kahru, S. A. Garver, McClain, C. R., 1998. Ocean color algorithms for SeaWiFS. J. Geophys. Res. 103, 24,937- 24,953.

O'Reilly, J. E., et al., 2000. Ocean color chlorophyll-a algorithms for SeaWiFS, OC2 and OC4, in: Hooker., S. B., Firestone, E. R. (Eds), SeaWiFS Postlaunch Calibration and Validation Analyses: Part 3, SeaWiFS Postlaunch Tech. Rep. Ser., pp. 9- 23.

Oubelkheir, K., Clementson, L.A., Webster,I.T., Ford, P.W., Dekker,A.G., Radke, L.C., Daniel, P., 2006. Using inherent optical properties to investigate biogeochemical dynamics in a tropical macrotidal coastal system. J. Geophys. Res. 111, 1-15.

Pandolfi, J.M., Bradbury, R.H., Sala, E., Hughes, T.P., Bjorndal, K.A., Cooke, R.G., McArdle, D., McClenachan, L. Newman, M.J.H., Paredes, G., Warner, R.R., Jackson, J.B.C., 2003. Global Trajectories of the Long-Term Decline of Coral Reef Ecosystems. Science 301, 955–958.

Parsons, T.R., Maita, Y., Lalli, C., 1984. A Manual of Chemical and Biological Methods for Seawater Analysis. Pergamon: London.

Petus, C. Chust, G., Gohin, F.,Doxaran, D., Froidefond, J.M., Sagarminaga, Y., 2010. Estimating turbidity and total suspended matter in the Adour River plume (South Bay of Biscay) using MODIS 250-m imagery. Cont. Shelf Res. 30, 379–392.

Pinet, P.R., 2000. Invitation to Oceanography, second ed. Jones and Bartlett Publishers, Boston, USA.

Qin, Y., Brando, V.E., Dekker, A.G., Blondeau-Patissier, D., 2007. Validity of SeaDAS water constituents retrieval algorithms in Australian tropical coastal waters. Geophys. Res. Lett. 34, L21603.

Saldías, G.S., Sobarzo, M., Largier, J., Moffat, C., Letelier, R., 2012. Seasonal variability of turbid river plumes off central Chile based on high-resolution MODIS imagery. Remote Sens. Environ. 123, 220–233.

Salyuk, P., Bukin, O., Alexanin, A., Pavlov, A., Mayor, A., Shmirko, C., Akmaykin, D., Krikun, V., 2010. Optical properties of Peter the Great Bay waters compared with satellite ocean colour data. Int. J. Remote Sens. 31, 4651-4664.

Schroeder, T., Devlin, M.J., Brando, V.E., Dekker, A.G., Brodie, J.E., Clementson, L.A., McKinna, L., 2012. Inter-annual variability of wet season freshwater plume extent into the Great Barrier Reef lagoon based on satellite coastal ocean colour observations. Mar. Pollut. Bull. 65, 210-23.

Titlyanov E.A., Latypov Y.Y., 1991. Light-dependence in scleractinian distribution in the sublittoral zone of South China Sea Islands. Coral Reefs 10, 133-138.

US EPA, Guidelines for Ecological Risk Assessment, 1998. U.S. Environmental Protection Agency, Risk Assessment Forum, Washington, D.C., EPA/630/R095/002F, 199 pp.

Wang, M.H., Shi, W., 2006. Cloud masking for ocean color data processing in the coastal regions. IEEE Geosci. Remote. S. 44, 3196-3205.

Wang, M., Shi, W., 2007. The NIR-SWIR combined atmospheric correction approach for MODIS ocean color data processing, Opt. Express 15, 15722-15733.

Waterhouse, J., Brodie, J., Lewis, S., Mitchell, A., 2012. Quantifying the sources of pollutants to the Great Barrier Reef. Mar. Pollut. Bull. 65, 394–406.

Wenger, A., McCormick, M. I., 2013. Determining trigger values of suspended sediment for behavioral changes in a coral reef fish. Mar. Pollut. Bull. 70, 73-80.

Wiseman Jr, W.J., Garvine, R.W., 1995. Plumes and Coastal Currents Near Large River Mouths. Estuaries 18, 509-517.

Weeks, S., Werdell, P.J., Schaffelke, B., Canto, M., Lee, Z., Wilding, J.G., Feldman, G.C., 2012. Satellite-Derived Photic Depth on the Great Barrier Reef: Spatio-Temporal Patterns of Water Clarity. Remote Sensing 4, 3781-3795.

Wolanski, E., Jones, M., 1981. Physical properties of Great Barrier Reef Lagoon waters near Townsville. I. Effects of Burdekin River Floods. Aust. J. Mar. Fresh. Res. 32, 305-319.

Wolanski, E., van Senden, D., 1983. Mixing of Burdekin river flood waters in the Great Barrier Reef. Aust. J. Mar. Fresh. Res. 34, 49–63.

Wolanski, E., Fabricius, K., Cooper, T. Humphrey, C., 2008. Wet season fine sediment dynamics on the inner shelf of the Great Barrier Reef. Estuar. Coast Shelf S.77, 755-762.